
PAC: A NOVEL SELF-ADAPTIVE NEURO-FUZZY CONTROLLER FOR MICRO AERIAL VEHICLES *

A PREPRINT

Md Meftahul Ferdous

School of Engineering and Information Technology
UNSW, Canberra, ACT
Australia, 2612
m.ferdaus@student.unsw.edu.au

Mahardhika Pratama

School of Computer Science and Engineering
Nanyang Technological University
Singapore, 639798
mpratama@ntu.edu.sg

Sreenatha G. Anavatti

School of Engineering and Information Technology
UNSW, Canberra, ACT
Australia, 2612
s.anavatti@adfa.edu.au

Matthew A. Garratt

School of Engineering and Information Technology
UNSW, Canberra, ACT
Australia, 2612
M.Garratt@adfa.edu.au

Edwin Lughofer

Department of Knowledge Based Mathematical Systems
Johannes Kepler University, Linz, Austria
edwin.lughofer@jku.at

October 9, 2019

ABSTRACT

There exists an increasing demand for a flexible and computationally efficient controller for micro aerial vehicles (MAVs) due to a high degree of environmental perturbations. In this work, an evolving neuro-fuzzy controller, namely Parsimonious Controller (PAC) is proposed. It features fewer network parameters than conventional approaches due to the absence of rule premise parameters. PAC is built upon a recently developed evolving neuro-fuzzy system known as parsimonious learning machine (PALM) and adopts new rule growing and pruning modules derived from the approximation of bias and variance. These rule adaptation methods have no reliance on user-defined thresholds, thereby increasing the PAC's autonomy for real-time deployment. PAC adapts the consequent parameters with the sliding mode control (SMC) theory in the single-pass fashion. The boundedness and convergence of the closed-loop control system's tracking error and the controller's consequent parameters are confirmed by utilizing the LaSalle-Yoshizawa theorem. Lastly, the controller's efficacy is evaluated by observing various trajectory tracking performance from a bio-inspired flapping wing micro aerial vehicle (BI-FWMAV) and a rotary wing micro aerial vehicle called hexacopter. Furthermore, it is compared to three distinctive controllers. Our PAC outperforms the linear PID controller and feed-forward neural network (FFNN) based nonlinear adaptive controller. Compared to its predecessor, G-controller, the tracking accuracy is comparable, but the PAC incurs significantly fewer parameters to attain similar or better performance than the G-controller.

Keywords Micro aerial vehicle · Neuro-fuzzy · Parsimonious learning machine · Self-adaptive

*This paper has been accepted for publication in Information Science Journal 2019. The source code is available in https://www.researchgate.net/publication/336241858_Code_hexacopter_PAC_latest.

1 Introduction

Advancements in portable electronic technology over the past few years encourage researchers to work on Micro Aerial Vehicles (MAVs). Attempts to humanize these MAVs, such as with the capacity of autonomous flying in a confined space is challenging. A positive step to such achievement is the low cost of miniature electronic components like sensors, actuators, microprocessors, batteries, etc. Another point is their immense applicability in both civilian and military sectors. Usage of MAVs in the military sector has intensified in the last decades. Participation of MAVs in civilian applications also has a lot of socio-economic benefits. To transmute all these potentialities of MAVs into reality, a major concern is to pursue the preferable control autonomy.

First principle techniques (FPTs) are prevalent in stabilizing and controlling MAVs, but, within a specific range around the equilibrium. Among numerous FPTs, linear controllers like Proportional Integral Derivative (PID), Linear Quadratic (LQ) methods are employed successfully in different MAVs due to straightforward structure. Nonetheless, linear controllers performance degrade abruptly to deal with environmental disruption due to MAV's inherent non-linearity and coupled dynamics. In rejecting disturbance of nonlinear MAV dynamics, nonlinear control techniques namely Backstepping, Sliding Mode techniques, Feedback Linearization (FBL), H_∞ perform diligently. A shortfall of all these linear and nonlinear controllers is their foremost dependency on the precise plant dynamics to be controlled. In MAVs, noisy data may obtain from various sensors and microelectronic components. Besides, encountering environmental disruptions like wind gust in open space, actuator degradation is usual in MAVs. Integration of such unexpected facts in MAV's dynamics is laborious or inconceivable. These deficiencies of FPT based controllers tempts research towards mathematical model-free methods.

Among numerous model-free approaches, the Fuzzy Logic systems (FLS), and Neural Networks (NN) are the most commonly used methods in various control applications [1], since they can effectively deal with complex nonlinear and chaotic systems. When superiority's of both FLS and NN based controllers are joined into a single structure, they are known as Neuro-Fuzzy (NF) controllers, which are also employed in diverse engineering industries. However, development of a NN, FLS or NF-based high-performance controllers is tough. Among numerous existing methods, a simple way to construct NN, FLS or NF-based controller is to train them offline using the known knowledge about the plant dynamics. Furthermore, it can be executed by mimicking an FPT controller like PID through offline training. These trained controllers possess several deficiencies. Firstly, they consist of a fixed architecture with an exact number of neurons or membership functions, rules or layers. With their static configuration, they can not adapt with time-varying non-stationary plants. Secondly, the controllers have a dependency on experts knowledge or training data. Therefore, control performance relies on the accuracy of that knowledge or data. To summarize, these static NN, FLS or NF-based controllers do not have any direct association with the plant models; rather, there exists an indirect reliance. To mitigate limitations of these static controllers, researchers have tried to utilize an adaptive neuro-fuzzy inference system (ANFIS) in various control applications [2, 3, 4, 5]. To improve the performance of the type-1 FLS, or type-1 ANFIS-based controllers, and to handle uncertainties, research has also been observed to develop type-2 FLS-based controllers [6, 7, 8, 9, 10].

To improve the performance of model-free static controllers, or ANFIS-based controllers, whether using type-1 or type-2 mechanism, researchers have developed adaptive controllers by combining conventional nonlinear control techniques such as backstepping, sliding mode techniques [11], feedback linearization (FBL), H_∞ , etc. with FLS, NN, or NF structure, which can tune their network parameters to alleviate the adverse influence of uncertainties and disturbances. In these control schemes, only the network parameters are altered, where they are maintaining a fixed structure. It enforces us to specify the number of nodes, layers, or rules beforehand. It is hard to know the exact number of rules a priori to attain the desired control performance. Controllers with only a few rules may fail to produce the desired performance, whereas too many of them may originate an over-complex structure of controllers to actualize in real-time. To circumvent such shortcomings, NN or NF controllers with flexible architecture can be employed. These flexible controllers are not only able to tune parameters, but also to evolve the structure by adding or deleting layers or rules in self-adaptive fashion [12]. In addition, the self-adaptive trait is capable of adapting to changing plant dynamics without re-tuning or retraining phase from scratch.

Research on evolving intelligent controllers has started at the beginning of the twenty-first century. In 2003, a self-organizing NF controller was proposed in [13], where they applied system error, ϵ -completeness, and error reduction ratio in their rule evolution scheme. Their controller needed to store all preceding input-output data, which forced to compute a large matrix in each step and yields a high computation cost. It makes them impractical to implement in systems like MAVs, where a fast response is expected from the controller to emulate the desired commands. Another evolving controller was developed in [12] by utilizing the evolving Takagi Sugeno (eTS) model [14]. Though their controller was evolving in nature, it suffers from several imperfections. First, in their structural evolution mechanism, fuzzy rules were added or replaced only, pruning of rules was missing. Besides, their eTS fuzzy controller needed to memorize the previous data obtained from both the plant and controller. Such limitation led to a computationally

costly control mechanism and made them unrealistic in swift reaction-based control application. A hybrid evolving controller was developed in [15] by mixing an evolving and a static TS-fuzzy system. Despite their design simplicity, they required to know some parameters of the plant to be controlled. Such parameters may not be available during control operation. An evolving controller was also actualized using model predictive control technique [16]. However, their dependency on plant's dynamic model restricted their application in complex nonlinear systems, where dynamic models may not be known.

Above mentioned evolving NN, FLS or NF-based controller are equipped with hyper-sphere-shaped clustering techniques, where mostly univariate Gaussian membership functions are used. As a consequence, those evolving controllers are associated with several rule premise parameters like mean and width. These parameters need to be updated continuously, which rises computational complexities. Recently, hyper-ellipsoid-shaped clustering-based evolving NF controller namely G-controller was developed by [17]. Multivariate Gaussian function was used due to its scale-invariant behavior and ability to handle both axis parallel and non-axis parallel data distribution. Nevertheless, like the hyper-sphere-shaped clustering-based counterparts, the G-controller involved numerous network parameters. A bottleneck of evolving controllers is the engagement of manifold parameters, which strikes adversely in furnishing a fast response. To lessen the parameters of evolving controllers, [18] used evolving data-cloud-based clustering technique to develop an evolving TS-fuzzy controller. Though they reduced network parameters, still bound to calculate accumulated distance of a particular point to all other points. The obligation of such calculation can not effectively diminish the memory demand of their evolving controller.

To mitigate the computational complexity of the above discussed evolving controllers, hyper-plane-shaped clustering technique-based evolving controller could be a promising avenue, since they are free from premise parameters. Lately, a hyper-plane-shaped clustering technique-based evolving NF architecture, namely parsimonious learning machine (PALM) was proposed in [19]. In this work, the PALM architecture has been utilized to develop an evolving controller namely PAC. Unlike the PALM, the rule adaptation module in PAC is replaced to originate a simplified evolving controller. In addition, the self-constructing clustering and similarity analysis-based rule-evolution mechanism of PALM have a dependency on user-defined parameters. To mitigate such dependency, in PAC, the rule evolution mechanism of PALM has been swapped with the so-called network significance method, which is deduced from the idea of bias-variance trade-off [20]. In PAC's rule evolution technique, the statistical contribution of each rule can be estimated to add or prune them on demand, which aids to achieve the desired control performance.

1.1 Main features

Main features of our proposed evolving controller, namely PAC can be uttered as follows:

1. **Premise-free fuzzy rule-based system:** Usually, fuzzy logic controllers are rule-based. They consist of antecedent and consequent parts, where both parts are associated with several parameters. Unlike the conventional fuzzy logic controller, the fuzzy rules in PAC are portrayed by hyper-planes which underpins both the rule premise and consequent parts. As a result, it does not have any premise parameter. Such scheme trims the rule-based parameters to the level of $R \times (N + 1)$, where N denotes the number of input dimension and R is the number of fuzzy rules. The number of network parameters of the proposed controller is considerably lower than the conventional evolving fuzzy controllers discussed in the literature.
2. **New rule growing and pruning mechanism based on bias and variance:** In PALM [19], self-constructing clustering approach was employed to generate rules, which faces computational complexities to calculate variance and covariance among different variables. Besides, similarity analysis among hyper-planes in terms of distance and orientation between hyper-planes were measured to merge rules in PALM. To eliminate such a complex calculation of growing and pruning rules, bias-variance concept-based simplified method, namely network significance [20] is proposed in PAC. A new rule is added in the underfitting situation, while the pruning process is triggered by the overfitting condition. The key difference of this paper from [20] lies in the estimation of bias and variance for the hyperplane-shaped clustering-based rules.
3. **New evolving fuzzy controller:** In general, the evolving fuzzy controllers' rule evolution methods have a reliance on a number of predefined thresholds. To eliminate such dependency on user-defined thresholds, the bias-variance concept based network significance method is exercised in PAC, where we do not need any user-defined problem-specific thresholds. Besides, the proposed controller has no premise parameters, its only consequent parameter, i.e., weights are adapted by using SMC learning theory to confirm a stable closed-loop system. To evaluate the controller's stable and precise tracking performance, it has been implemented into a simulated BI-FWMAV and hexacopter plant.

Aforementioned features of the PAC are desiring to achieve the desired control autonomy in MAVs. Therefore, the proposed controller is applied to control a BI-FWMAV and a hexacopter plant in this work. In addition, the whole code

of the PAC is written in C programming language. It is compatible with the majority of the MAVs hardware, where its implementation is made accessible publicly in [21] to assure reproducible research.

2 Related work

Recent advent in portable microelectronic technology is encouraging to develop MAVs. Their autonomous flying ability in both natural and human-made environment is aspiring for numerous defense applications. Besides, they can play a vital role in civilian ventures like disaster alleviation, communication, environment conservation, etc. Until now, majority of the commercially available MAVs are controlled by FPT-based linear controllers like PIDs because of their design simplicity and easy employment. In this work, we are dealing with the control performance of a hexacopter and BI-FWMAV. In regulating rotary wing and flapping wing MAVs, implementations of PID controllers have witnessed profusely in last decades. Though PIDs can control MAVs with satisfactory accuracy in certain environment, due to their fixed gain, they are not robust against real-world uncertainties like a wind gust. Another prominent linear control method for MAVs is Linear Quadratic (LQ) technique [22]. These linear controllers suffer from attaining desired performance due to the complex nonlinearity in system dynamics. Besides, various un-modeled uncertainties and perturbations have a detrimental influence on these precise-model-based linear controllers. Afterward, to control MAVs researchers had focused on various nonlinear controllers namely back-stepping, sliding mode control [23], feedback linearization (FBL), H_∞ robust control techniques by the virtue of their disturbance rejection. However, like their linear counterparts, nonlinear controllers have a direct association with the precise dynamic model to be controlled. Such dependency limits their application where the plant dynamics are unknown. In our work, the entire dynamics of the BI-FWMAV is unidentified, where exercising the model-based nonlinear controllers is impractical. Besides, BI-FWMAV's lightweight architecture is naive to manifolds un-modeled outdoor uncertainties. Model-free control approaches are an effective solution to deal with un-modeled uncertainties.

Model-free control approaches for MAVs have commenced with FLS [24], NN [25], or NF-based controllers [26]. However, the requirement of offline training, static structure, dependency on experts' knowledge confine their applicability in complex systems with the uncertain environment. Also, they experienced a spillover effect. To mitigate such shortcomings, researchers have tried to develop FLS, NN, and NF-based intelligent adaptive controllers [3, 5, 9]. However, these controllers are not able to alter their structure.

The evolving intelligent controllers have the promising quality to handle complex dynamic systems with uncertainties. Nonetheless, they have not yet been employed profusely in regulating MAVs due to the complex framework and challenging execution. Apart from that, MAVs require a control method with prompt response, which sometimes difficult to acquire from evolving controllers due to their high memory demand. Lately, an evolving controller using interval type-2 (IT2) NF structure was proposed in [27] to control a quadcopter MAV. Nonetheless, their IT2NF system was functioning as an uncertainty and perturbation observer, and a PD controller was used to control the attitude and position of the quadcopter. In [28], an evolving NF controller was proposed for a simulated quadcopter MAV plant. Though their controller successfully generated and pruned fuzzy rules on the fly with a satisfied tracking accuracy, they only had considered a simplified dynamic model of the quadcopter to be controlled. One of the latest research on evolving controller in regulating MAVs attitude and altitude was reported in [17]. Unlike the evolving controllers discussed in the literature, they effectually exercised a NF evolving controller in a high dimension nonlinear complex MAV plant. Besides, their controller was evaluated by incorporating uncertain wind gust effect in their MAVs plant. A comprehensive survey of evolving fuzzy system for regression, classification and control tasks is provided in [29].

In evolving controllers, the adaptation of consequent parameters plays a crucial role to attain the desired accuracy. To adapt the evolving controller's rule consequent parameters, gradient-based methods are typically used [30]. However, the gradient-based controllers perform well only when they were used to control plants with a slow variation in dynamics. Furthermore, gradient-based methods like dynamic back-propagation comprise of partial derivatives. Such algorithms can not guarantee fast convergence speed, particularly in complex non-convex search space. Also, there are chances to be trapped in a local minimum. Alternately, evolutionary algorithms were attempted in [31] to tune parameters. Nevertheless, the stability of their proposed controller was not confirmed, and the fast response was not ensured. Such constraints can be handled simply by imposing SMC theory to adapt the consequent parameters as witnessed in [17]. Inspired by the simplicity of the SMC theory [17], in our work, it has been employed to update the consequent parameters. Like [17], predefined static sliding parameters are replaced with learning rate based self-organizing parameters. It makes the proposed PAC a complete self-adaptive model-free controller.

Arrangement of the remaining sections of this paper is as follows: In Section 3, limitations of existing evolving controllers are analyzed. Section 4 details the network structures of the PALM-based evolving controller PAC along with the explanation on rule generation and pruning mechanism. Challenges in formulating FW AMV or hexacopter

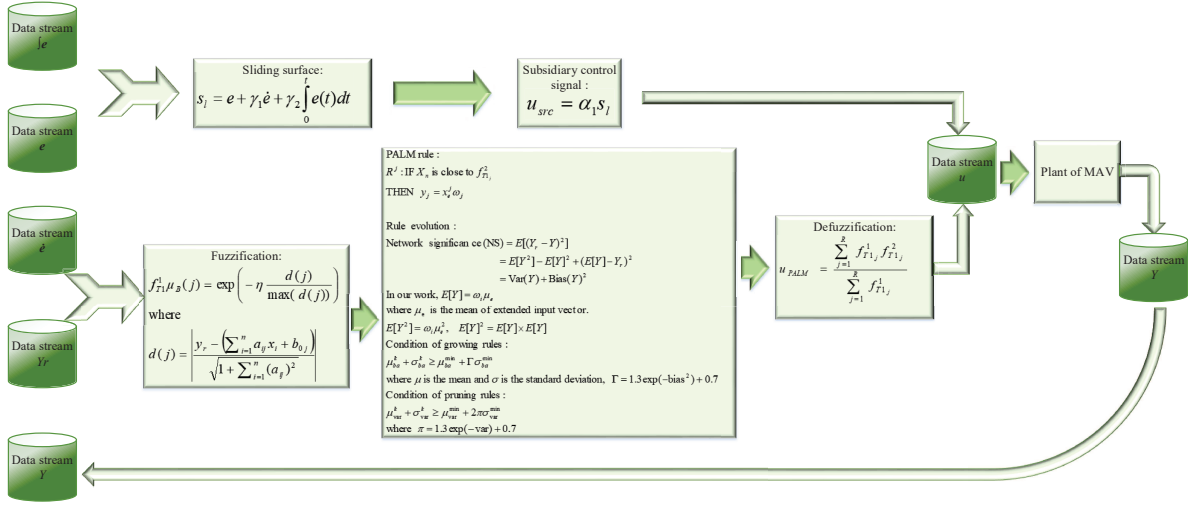


Figure 1: Flow of data streams in closed-loop PAC

model have asserted in Section 5. Experimental results and performance evaluation of the proposed controller are described in Section 6. The concluding remarks are drawn in Section 7.

3 Problem statement

In a closed-loop control system, data comes in a sequential online manner to the controller, which may contain various uncertainties and disturbances. Such an irregularly distributed sequence of incoming data to the controller can be exposed formally as $e = \{e^1, e^{1+t}, e^{1+2t}, \dots, e^f\}$, denoted by "Data steam of e " in Fig. 1, where t is the time step (in sec) of the closed-loop control system, f is the final time until which plants need to be controlled. Here, e is indicating the data stream of error, which is the difference between the reference trajectory data stream Y_r and observed corresponding out data stream from the plant Y . The remaining incoming data streams to the closed-loop system, as displayed in Fig. 1, are data streams of derivative of error (\dot{e}) and the integral of error ($\int e$). To tackle irregular sequence of incoming data, the controller should hold some desiring features such as 1) able to work in single-pass mode; 2) deal with various uncertainties of the incoming data; 3) perform with low memory burden and computational complexity to enable real-time deployment under resource-constrained environment. In the realm of NF systems, such learning proficiency is manifested by evolving NF systems [32]. However, enormous free parameters associated with the evolving NF controllers may cause complex computation. From the perspective of controlling MAV, a swift response from the controller is much expected, where tuning of several premise parameters in the evolving controller is a hindrance to fulfill such expectation. To decipher the involvement of profuse premise parameters in evolving controller, their premise parameter-dependent hyper-spherical or hyper-ellipsoidal clustering techniques can be substituted with premise parameter-free clustering method. From this research gap, a hyper-plane-based clustering method [19] is utilized in our work, which is composed from the consequent parameters as explained in [19]. Another inadequacy of state of the art evolving controllers is their affiliation to user-defined parameters to evolve their structure. Those parameters claim to alter with respect to the corresponding closed-loop system. Our proposed evolving controller is free from such parameters, and they have been superseded by the bias-variance concept. To get a clearer view, the flow of data streams in our closed-loop system is displayed in Fig. 1. Unlike the PALM [19], in the fuzzification layer of PAC, we always have incoming target/reference data stream Y_r as shown in the fuzzification block of the Fig. 1. Therefore, we have not used the recurrent PALM (rPALM) architecture like [19], since it does not have any access to the target value in the testing phase. To obtain an explicit impression, the self-evolving formation of our proposed PAC is enumerated in the next section.

4 Proposed parsimonious controller

Our proposed PAC is a three-layered NF system and functioning in tandem. It's evolving architecture is rooted with TS-fuzzy model, where classical hyper-spherical [12], hyper-ellipsoidal [33], or data-cloud based [18] clusters are substituted with hyper-plane-based clusters. Utilization of hyper-planes has removed antecedent parameters as explained in [19], which reduces the number of operative parameters in our controller dramatically. Popular hyper-plane-based clustering techniques procedures like fuzzy C-regression model (FCRM) [34], fuzzy C-quadratic shell (FCQS), double FCM [35], inter type-2 fuzzy c-regression model (IT2-FCRM) [36] are non-incremental in nature, thereupon can not entertain evolving hyper-planes. Additionally, they deployed hyper-spherical function for instance Gaussian function to accommodate hyper-planes. To mitigate such inadequacies, a new membership function [36] is used in PAC. To fetch a vivid overview of the mechanism of PALM itself, the architecture of the PALM network is detailed in the following subsection.

4.1 Architecture of PAC

In our PAC's closed-loop control system, the PALM network is fed by three inputs namely error (e), the derivative of error (\dot{e}) and actual plants output (y). Referring to the theory of fuzzy system, these crisp data (e, \dot{e}, y) need to be transformed into a fuzzy set, which is the initial step in the PALM's workflow. This fuzzification process is accomplished by adopting a new membership function that can adopt the hyper-plane-shaped clusters directly, which is framed through the concept of point-to-plane distance. The employed membership function can be expressed as follows:

$$f_{T1}^1 = \mu_B(j) = \exp\left(-\eta \frac{d(j)}{\max(d(j))}\right) \quad (1)$$

where η is a regulating parameter which adjusts the fuzziness of membership grades. Based on the observation in [36, 19], and empirical analysis with different MAV plants in our work, the range of η is fixed as [1, 100]. This membership function empowers the utilization of hyper-plane-based clusters directly into the PALM network without any rule parameters except the first-order linear function or hyperplane. In the proposed membership function, the calculation of the distance from a point to plane is not unique, where the compatibility measure is executed using the minimum point to plane distance. $d(j)$ in Eq. (1) denotes the distance between the current data point and j th hyperplane as with Eq. (2). It is determined by following the definition of a point-to-plane distance [37] and is formally expressed as follows [19]:

$$d(j) = \left| \frac{y_r - (\sum_{i=1}^n a_{ij}x_i + b_{0j})}{\sqrt{1 + \sum_{i=1}^n (a_{ij})^2}} \right| \quad (2)$$

where a_{ij} and b_{0j} are consequent parameters of the j th rule, $i = 1, 2, \dots, n$; n is the number of input dimension, and y_r is the reference trajectory to the plant. In the closed-loop control perspective, the target value y_r for the plant is always known. However, in the regression or classification problem, it is not possible to acquire the target value in the testing phase. Therefore, in [19], the target-value dependent PALM was advanced to a recurrent structure namely rPALM. Such recurrent architecture is not required in PAC since the target trajectory y_r is continually available up to the end of control performance. It is noteworthy to state that a type-1 fuzzy structure is facilitated in PAC. In light of a MISO system, the IF-THEN rule of PAC can be exposed as follows:

$$R^j : \text{ IF } X_n \text{ is close to } f_{T1_j}^2 \text{ THEN } y_j = x_e^j \omega_j \quad (3)$$

where x_e is the extended input vector and is expressed by inserting the intercept to the original input vector as $x_e = [1, e, \dot{e}, y]$, e is the error, i.e. the difference between the reference and actual output of the plant, \dot{e} is the error derivative, i.e. the difference between the present and previous state error value, y_r is the reference trajectory for the plant to be controlled, ω_j is the weight vector for the j th rule, y_j is the consequent part of the j th rule. The antecedent part of PAC is simply the hyperplane and does not consist of any premise parameters. From Eq. (3), it is observed that the drawback of PAC lies in the high-level fuzzy inference scheme which lowers the transparency of fuzzy rule. The intercept of extended input vector dominates the slope of hyperplanes which eliminates the untypical gradient dilemma.

In PAC, an analogous consequent part alike the basic TS-fuzzy model's rule consequent part ($y_j = b_{0j} + a_{1j}x_1 + \dots + a_{nj}x_n$) is employed. The consequent part for the j th hyperplane is calculated by weighting the extended input variable (x_e) with its corresponding weight vector as follows:

$$f_{T1_j}^2 = x_e^T \omega_j \quad (4)$$

The weight vector in Eq. (4) is updated recursively by the SMC theory-based adaptation laws, which ensures a smooth alteration in the weight value. In the next step, the rule firing strength is normalized and added with the rule consequent

to produce the end-output of PALM. The final defuzzified crisp output of the PALM can be expressed as follows:

$$u_{PALM} = \frac{\sum_{j=1}^R f_{T1_j}^1 f_{T1_j}^2}{\sum_{i=1}^R f_{T1_i}^1} \quad (5)$$

The normalization term in Eq. (5) assures the partition of unity where the sum of normalized membership degree is one. The above-described PALM network-based PAC has a similar structure like [19]. Nonetheless, a simplified learning mechanism is used in PAC than the original PALM, as explained in the next subsection.

4.2 Automatic constructive mechanism of PAC

In PALM [19], the self-constructive clustering technique was adopted to grow the rules. The rule-significance was determined by measuring input and output coherence, where the coherence was calculated by investigating the correlation between the existing data samples and the target concept. Again, the computation of correlation has a dependency on finding variance and covariance among different variables. In addition, the PALM's rule growing method was regulated by two predefined thresholds. PALM's rules were merged by measuring the similarity between the hyperplane-shaped fuzzy rules. The similarity among rules was measured by observing the angle and minimum distance among them. The merging strategy was also controlled by predefined thresholds. This clearly shows the high computational cost of PALM's rule evolving mechanism and made them incompatible in fast response-based control applications. To subjugate such complexity, a simplified rule evolution technique is implemented in PAC bottomed by the network significance method, which is formulated from the concept of bias-variance [20]. Here, no predefined thresholds are required to regulate the generation or pruning of the fuzzy rules. This network significance method based rule growing and deletion modules of PAC are clarified in subsequent paragraphs of this section.

4.2.1 New Mechanism of rule generation in PAC

The strength of PAC can be analyzed by considering the tracking error, which can be written in terms of mean square error (MSE) as follows:

$$MSE = \sum_{t=1}^T \frac{1}{T} (y_r(t) - y(t))^2 \quad (6)$$

where $y_r(t)$ is expressing the desired trajectory and $y(t)$ is attained output from the plant to be controlled. Such formulation experiences two obstructions in the learning mechanism of an evolving controller, such as 1) it needs to memorize all data points to get a clearer view about the controller's constructive mechanism; 2) though the recursive calculation of MSE by excluding preceding data is possible, it does not investigate the strength of reconstruction for uncertain upcoming data. In simple words, it does not consider the generalization capacity of evolving controllers. To mitigate such hindrance, let us consider that $Y(t)$ is the observed plant's output for the reference input $Y_r(t)$, and $E[Y(t)]$ is the plant's expected output. According to the definition of expectation, if x is continuous, then the expectation of $f(x)$ can be formulated as $E[f(x)] = \int_{-\infty}^{\infty} f(x)p(x)dx$, where $p(x)$ is the probability density function of x . Then the network significance (NS) method can be defined as follows:

$$NS = \int_{-\infty}^{\infty} (Y(t)_r - Y(t))^2 p(t)dt \quad (7)$$

where $p(t)$ is denoting the probability density function of t . In effect, the NS method is the expectation of squared tracking error, and verbalized as follows:

$$NS = E[(Y_r(t) - Y(t))^2] = E[(Y(t) - E[Y(t)] + E[Y(t)] - Y_r(t))^2] \quad (8)$$

After several mathematical operations, NS can be formulated with the concept of bias and variance as follows:

$$NS = E[(Y(t) - E[Y(t)])^2] + (E[Y(t)] - Y_r(t))^2 = \text{Var}(Y(t)) + \text{Bias}(Y(t))^2 \quad (9)$$

In Eq. (9), the variance of $Y(t)$ i.e., $\text{Var}(Y(t))$ can be presented as follows:

$$\begin{aligned} \text{Var}(Y(t)) &= E[(Y(t) - E[Y(t)])^2] = \int_{-\infty}^{\infty} (Y(t) - E[Y(t)])^2 p(t)dt \\ &= E[Y(t)^2] - E[Y(t)]^2 \end{aligned} \quad (10)$$

In establishing the NS in PAC, a rule firing strength of unity is assumed. It simplifies the network outcome as $Y(t) = \sum_{i=1}^R x_e \omega_i$, because the expectation of the normalized firing strength of PAC does not have a unique

solution. Here x_e is the extended input and can be exposed as $x_e = [1, x_1, x_2, \dots, x_n]$, where n is the number of inputs to the network; ω_i is the weight vector of the i th rule. Now the expectation of Y can be formulated as $E[Y(t)] = \int_{-\infty}^{\infty} x_e \omega_i p(t) dt$. Suppose that the normal distribution applies, it leads the expectation to the following expression.

$$E[Y(t)] = \omega_i \mu_e \quad (11)$$

where μ_e is mean of the extended input x_e . Factually, the integration of x_e over $-\infty$ to ∞ originates the mean μ_e .

Let us call back the formula of variance $\text{Var}(Y(t)) = E[Y(t)^2] - E[Y(t)]^2$, where the second term of the right-hand side is simply $E[Y(t)]^2 = E[y(t)] \times E[y(t)]$, and the first term can be formulated as $E[Y(t)^2] = \omega_i \mu_e^2$. Incorporation of all these results in NS formula of Eq. (9) settles the final manifestation of NS. Since the NS consists of both bias and variance, a high value of NS may indicate a high variance (over-complex network with profuse fuzzy rules) or a high bias (oversimplified network) problem. Such phenomenon can not be elucidated simply by system error index. Augmentation of a new rule is inferred to subjugate the high bias dilemma. Nonetheless, such phenomenon is not convenient for high variance context since the addition of rules magnifies the network complexity. To retain a compact network structure with satisfactory tracking performance, the concept of bias-variance trade-off is inserted in our work to calculate the NS [38, 20]. Therefore, the rule-evolution of our controller has no reliance on user-defined parameters. By confirming the fundamental objective of rule growing procedure to ease the high bias dilemma, the condition of growing rules in our work is expressed as follows:

$$\mu_{ba}^k + \sigma_{ba}^k \geq \mu_{ba}^{min} + \Gamma \sigma_{ba}^{min} \quad (12)$$

where μ_{ba}^k is denoting the mean of bias and σ_{ba}^k is the standard deviation of bias at the k th observation while μ_{ba}^{min} and σ_{ba}^{min} are pointing the minimum of mean and standard deviation up to k th time instant. In computing these variables, no preceding data are required. Their values are being updated directly based on the availability of upcoming signals to the PAC. When Eq. (12) is satisfied, the values of μ_{ba}^{min} and σ_{ba}^{min} are to be reset. To perceive an improved tracking performance from the commencing of PAC's control operation, a rapid decay in the bias value is expected. It is retained in formulating the settings of bias in Eq. (12) as long as the plant does not encounter any uncertainties or disturbances. The presence of any disruptions in control system will elevate value of bias, which cannot be addressed directly by adapting the consequent parameter of the PAC. To elucidate such hindrance, Eq. (12) is originated from the adaptive sigma rule, where Γ controls the degree of confidence of the sigma rule. In our work, the Γ is expressed as $\Gamma = 1.3 \exp(-\text{bias}^2) + 0.7$, which revolves Γ between 1 and 2. Consequently, it obtains the level of confidence from around 68% to 96%. Such scheme enhances the flexibility in the rule-growing module to adapt to environmental perturbations. It also eliminates the dependency of evolving controller on user-defined problem-dependent parameters. To sum up, a high bias usually signifies an oversimplified network, which is solved by adding rules. However, it is avoided in case of low bias since it may magnify the variance. (12) follows the statistical process control approach [39, 40] where the modification here exists in the use of dynamic Γ .

4.2.2 New rule pruning module of PAC

The structure of PAC may become highly complex as a result of high variance. On that ground, control of variance is essential to reduce the network complexity by pruning the fuzzy rules. Since a high variance indicates the overfitting condition, the rule pruning scheme initiates from the evaluation of variance. Like the rule growing mechanism of PAC, a statistical process control technique [40] with dynamic confidence level is embraced in rule pruning module to trace the high variance dilemma as follows:

$$\mu_{var}^k + \sigma_{var}^k \geq \mu_{var}^{min} + 2\pi \sigma_{var}^{min} \quad (13)$$

where μ_{var}^k is denoting mean and σ_{var}^k is the standard deviation of variance at the k th observation while μ_{var}^{min} and σ_{var}^{min} are pointing the minimum of mean and standard deviation up to k th time instant. Here, the term π is adopted as $\pi = 1.3 \exp(-\text{var}) + 0.7$, π is a dynamic constant and regulating the degree of confidence in the sigma rule. The term 2 is Eq. (13) halts the direct pruning after growing. Furthermore, μ_{var}^{min} and σ_{var}^{min} are reset when the condition in Eq. (13) is fulfilled.

After the execution of Eq. (13), the significance of each rule is examined via the idea of network significance, and inconsequential rules are pruned to reduce the overfitting condition. The significance of the i th rule is determined by its average activation degree for all possible incoming data samples or its expected values as expressed in Eq. (9). Considering the normal distribution assumption, the importance of i th rule can be expressed as $HS_i = \omega_i \mu_e$. A small value of HS_i indicates that the i th rule plays a small role to recover the clean input attributes. Therefore, it can be pruned with a very insignificant loss of tracking accuracy. Since the contribution of the i th rule is calculated in terms of the expectation $E(Y)$, the least contributing rule having the lowest HS is regarded inactive. When the overfitting condition occurs or Eq. (13) is satisfied; the rule with the lowest HS is pruned and can be expressed as follows:

$$\text{Pruning} \longrightarrow \min_{i=1, \dots, R} HS_i \quad (14)$$

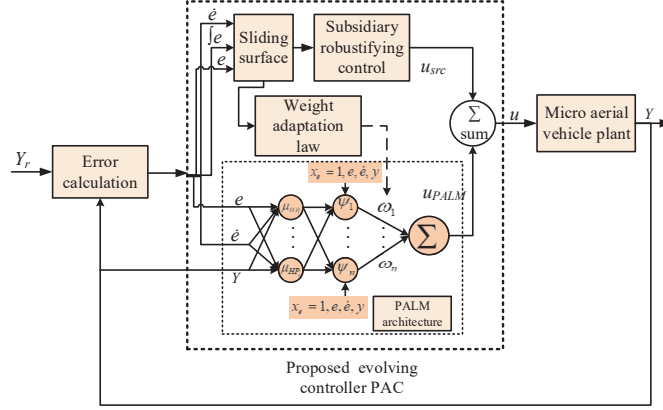


Figure 2: Self-adaptive PAC's closed-loop mechanism

The condition in Eq. (14) targets to mitigate the overfitting situation by deleting the least significant rule. It also indicates that the desired trajectory tracking performance can still be achieved with the rest $R - 1$ rules. Furthermore, this rule pruning strategy enhances the generalization power of PAC by reducing its variance, which helps to deal with a variety of disturbances.

4.3 Adaptation of weights in PAC

Unlike the conventional evolving controllers, PAC does not possess any premise parameter, consequently free from the computation of tuning those parameters. PAC's consequent parameter namely Weight needs to be adjusted to realize the desired control efficacy. Inspired by the smooth employment and regulations of SMC theory in various neuro-fuzzy systems [41, 42, 43], in our work, SMC learning theory is functioned to adapt the PAC's weight, which ascertains the boundedness of the tracking error in the closed-loop control system. Besides, it confirms adequate robustness in a system against exterior obstructions, parameter variations, and uncertainties [17]. In designing the SMC, a time-varying *sliding surface* that restricts motion of a system to a plane can be exposed as follows:

$$S_{ss}(u_{PALM}, u) = u_{src}(t) = u_{PALM}(t) + u(t) \quad (15)$$

In this work, the sliding surface for BI-FWMAV and hexacopter plants to be controlled can be expressed as:

$$s_l = e + \gamma_1 \dot{e} + \gamma_2 \int_0^t e(t) dt \quad (16)$$

where, $\gamma_1 = \frac{\alpha_2}{\alpha_1}$, $\gamma_2 = \frac{\alpha_3}{\alpha_1}$, e is the error, i.e., the divergence from the trajectory obtained from the plant to the reference one. Here, the sliding parameters are initiated with small values such as $\alpha_1 = 1 \times 10^{-2}$, $\alpha_2 = 1 \times 10^{-3}$, $\alpha_3 \approx 0$. These parameters are further evolved by using dissimilar learning rates. Proper assignment of these rates supports to secure the desired parameters with minimal time, which affirms to gain stability in the closed-loop system swiftly. Engagement of these self-organizing sliding parameters shapes a fully model-free controller. Similar definition as of G-controller [17] is maintained in this work as follows:

Definition : After a specific time t_k , a sliding motion will be formed on the sliding manifold $S_{ss}(u_{PALM}, u) = u_{src}(t) = 0$, where the state $S_{ss}(t)\dot{S}_{ss}(t) = u_{src}(t)\dot{u}_{src}(t) < 0$ to be convinced for the entire period with some non-trivial semi-open sub-interval of time expressed as $[t, t_k) \subset (0, t_k)$.

To enforce the above-mentioned definition of sliding mode condition, the weights of the proposed PAC are adapted accordingly.

In our proposed controller, the reliance of the subsidiary robustifying control term on the sliding surface can be formulated as follows:

$$u_{src}(t) = \alpha_1 s_l \quad (17)$$

This subsidiary robustifying control term u_{src} may endure high-frequency oscillations in contributing to the control input. Such repulsive occurrence in sliding mode control theory is termed as chattering effect. To suppress this

chattering effect, control systems are primarily facilitated with saturation or sigmoid functions. In this work, due to simplicity, a saturation function is used to alleviate those detrimental consequence.

The outcome from PALM (u_{PALM}) in PAC can be expressed as follows:

$$u_{PALM}(t) = \psi^T(t)\omega(t) \quad (18)$$

The overall control signal as observed in Fig. 2 can be declared as follows:

$$u(t) = u_{src}(t) - u_{PALM}(t) \quad (19)$$

Theorem 1. *The adaptation law to guarantee the boundedness of the tracking error and the consequent parameter, i.e. weights of PAC is expressed as:*

$$\dot{\omega}(t) = -\gamma \mathbf{e} P b \psi \quad (20)$$

where $\gamma > 0$, P is a positive definite matrix as exposed in Eq. (31), b is an unknown positive constant, $\mathbf{e} = [e \ \dot{e}]$. These weight adaptation laws assure a stable closed-loop control system.

4.3.1 Proof of boundedness of error and weights in PAC

Proof : Let us consider a n th order nonlinear system of the form as follows:

$$X^{(n)} = F(X, \dot{X}, \dots, X^{(n-1)}) + bu, \quad Y = X \quad (21)$$

where $F(\cdot)$ is an unknown continuous function, b is an unknown positive constant. $u \in \mathfrak{R}$ is the input and $Y \in \mathfrak{R}$ is the output of the system. We have considered that the state vector $\mathbf{X} = (X_1, X_2, \dots, X_n)^T = (X, \dot{X}, \dots, X^{(n-1)})^T \in \mathfrak{R}^n$ is available for measurement. Our control objective in this work is to push Y to track a given reference trajectory Y_r . To be specific, the control objectives can be summarized as follows:

- i) Parameters of the closed-loop control system should be uniformly ultimately bounded to confirm the global stability of that closed-loop system. In this work, $|\mathbf{X}(t)| \leq M_{\mathbf{X}} < \infty$, $|\omega(t)| \leq M_{\omega} < \infty$, and $|u(\mathbf{X}|\omega)| \leq M_u < \infty$ for all $t \geq 0$, where $M_{\mathbf{X}}$, M_{ω} , and M_u are pre-defined design parameters.
- ii) The closed-loop tracking error $e = Y_r - Y$ should be as small as possible by satisfying the conditions in i.

Our proposed PAC should be able to achieve these control objectives. To show that, let us consider $\mathbf{e} = (e, \dot{e}, \dots, e^{(n-1)})^T$ and $\mathbf{k} = (k_1, \dots, k_n)^T \in \mathfrak{R}^n$ carry such features that all roots of the polynomial $h(p) = p^n + k_1 p^{(n-1)} + \dots + k_n$ will be in the open left-half plane. If we know about the function $F(\cdot)$ and constant b , then the optimal control law for PAC can be expressed as follows:

$$u^* = \frac{1}{b} [-F(\mathbf{X} + Y_r^{(n)} + \mathbf{k}^T \mathbf{e})] \quad (22)$$

Now, applying the optimal control law of Eq. (22) in Eq. (21) yields the follows:

$$e^{(n)} + k_1 e^{(n-1)} + \dots + k_n e = 0 \quad (23)$$

From Eq. (23), it is obvious that $\lim_{t \rightarrow \infty} e(t) = 0$, which is the desired control objective from the proposed controller. Since both $F(\cdot)$ and b are unknown, the optimal control law cannot be implemented. In such circumstance, PALM is used to approximate the optimal control law. Now utilizing Eq. (19) in Eq. (21), the following is obtained:

$$X^{(n)} = F(\mathbf{X}) + b[u_{src} - u_{PALM}] \quad (24)$$

By following the approach in [44], bu^* is added and subtracted to Eq. (24). After several modification, the error equation governing the closed-loop system can be exposed as follows:

$$e^n = -k^T \mathbf{e} + b[u_{src} - u_{PALM}] \quad (25)$$

By following the approach of [44, 45], the error dynamics in our work can be presented as follows:

$$\dot{\mathbf{e}} = \mathbf{Ae} + b(u_{PALM} - \epsilon) \quad (26)$$

where $\mathbf{e} = [e \ \dot{e}]^T$, $A = \begin{bmatrix} 0 & 1 \\ -\alpha_1 & -\alpha_2 \end{bmatrix}$, and $b = [0 \ 1]^T$. Let us denote an ideal weight as ω^* by defining the corresponding weight error as $\tilde{\omega} = \omega - \omega^*$. Now, the error dynamics can be rewritten as:

$$\dot{\mathbf{e}} = A\mathbf{e} + b\psi^T \tilde{\omega} + b(\psi^T \omega^* - \epsilon) \quad (27)$$

Assume that, in the domain of interest, the ideal weight brings the term $\psi^T(t)\omega^*(t)$ to within a Δ -neighbourhood of the error ϵ . It is bounded by

$$\Delta^* \equiv \sup_z |\psi^T(z)\omega^* - \epsilon(z)| \quad (28)$$

where z is the vector that contains all the variables of the inversion error. The term $|\psi^T(z)\omega^* - \epsilon(z)|$ represents a residual inversion error which is not modeled by the PAC. Therefore, Δ^* is defined as the worst-case difference between the error and its best approximation.

In this work, the considered candidate Lyapunov function is as follows:

$$V = \frac{1}{2} \mathbf{e}^T P \mathbf{e} + \frac{1}{2\gamma} \tilde{\omega}^T \tilde{\omega} \quad (29)$$

where $\gamma > 0$. For $\alpha_1 > 0$ and $\alpha_2 > 0$, A in Eq. (26) is Hurwitz, P is a positive definite matrix and satisfying the following equation:

$$A^T P + P A = -Q \quad (30)$$

where $Q > 0$. For all $Q > 0$, the solution of Eq. (30) is > 0 . For $Q = I_2$, it is implying the following value of P :

$$P = \begin{bmatrix} \frac{\alpha_2}{\alpha_1} + \frac{1}{2\alpha_2} & \frac{1}{2\alpha_1} \\ \frac{1}{2\alpha_1} & \frac{1+\alpha_1}{2\alpha_1\alpha_2} \end{bmatrix} \quad (31)$$

Now, the time derivative of the Lyapunov function V with the substitution of Eq. (26) and Eq. (30) can be expressed as:

$$\dot{V} = -\frac{1}{2} \mathbf{e}^T Q \mathbf{e} + \mathbf{e}^T P b (\psi^T \omega^* - \epsilon) + \tilde{\omega}^T (t) (\mathbf{e}^T P b + \frac{1}{\gamma} \dot{\tilde{\omega}}) \quad (32)$$

The third term of Eq. (32) is suggesting a design of the adaptation law as follows:

$$\dot{\tilde{\omega}} = \dot{\omega} = -\gamma \mathbf{e}^T P b \psi \quad (33)$$

After employing the above adaptation law to Eq. (32), it can be reduced as:

$$\dot{V} = -\frac{1}{2} \mathbf{e}^T Q \mathbf{e} + \mathbf{e}^T P b (\psi^T \omega^* - \epsilon) \leq -\frac{1}{2} \|\mathbf{e}\|_2^2 + \Delta^* |\mathbf{e}^T P b| \quad (34)$$

Utilizing the inequality exposed in [45], we can write:

$$\mathbf{e}^T P \mathbf{e} \leq \bar{\lambda}(P) \|\mathbf{e}\|_2^2 \quad (35)$$

Using Eq. (35), the following is obtained from Eq. (34):

$$\dot{V} \leq -\frac{\mathbf{e}^T P \mathbf{e}}{2\bar{\lambda}(P)} + \Delta^* \sqrt{\mathbf{e}^T P \mathbf{e}} \sqrt{\bar{\lambda}(P)} \quad (36)$$

Equation (36) is strictly negative when:

$$\sqrt{\mathbf{e}^T P \mathbf{e}} > 2\Delta^* (\bar{\lambda}(P))^{3/2} \quad (37)$$

According to the LaSalle-Yoshizawa theorem, since \dot{V} is strictly negative, it is sufficient to prove that \mathbf{e} and $\omega(t)$ will be remained bounded. In addition, if $\Delta^* = 0$, there will be no approximation error, then $e(t) \rightarrow 0$ as $t \rightarrow \infty$. It is guaranteeing the asymptotic stability of the system.

Unlike the conventional neuro-fuzzy systems, consequent parameters, namely weights of PAC, are also utilized in the antecedent part as exposed in Eq. (2). Therefore, it is important to confirm the boundedness of the weights while they were used in the antecedent part. In this work, the weights are initialized with small values (less than one). Then, they are updated recursively, where their boundedness is confirmed and explained in the above paragraphs. Absolute value is considered in the distance formula since the distance cannot be negative. The calculated distance from the weights is employed in the fuzzification layer. In Eq. (1), η is a positive constant, the highest value for the ratio between the distance and maximum distance is one and positive. Therefore, the values for the exponent operator always remains negative and bounded by η , which confirms the stability of the antecedent part of the PAC.

5 Plant dynamics of MAVs

Both hexacopter and BI-FWMAV plants were developed at UAV laboratory of the UNSW Canberra, where development of the BI-FWMAV plant was inspired by the work of [46, 47]. These plants are used in our work to evaluate the proposed PAC's performance. In this section, we are initiating with hexacopter's nonlinear complex plant dynamics.

5.1 Dynamics of hexacopter plant

Rigid body dynamics of our hexacopter plant is formulated using Newton's second law of motion, where we have calculated correlations between the forces and moments acting on the hexacopter and translational and rotational accelerations. We have assumed our hexacopter plant as a traditional mass distribution, where the plane of symmetry was XZ plane. Such consideration makes the cross product of moments of inertia in YZ and XY plane zeros. After this simplified implementation, the equations of forces (F_x, F_y, F_z) and moments (L, M, N) in X, Y and Z axes are exposed in Eq. (38). For further clarifications, readers can go through [48], where equations in (38) are derived elaborately.

$$\begin{aligned}
 F_x &= m(\dot{u} + qw - rv) \\
 F_y &= m(\dot{v} + ru - pw) \\
 F_z &= m(\dot{w} + pv - qu) \\
 L &= I_x \dot{p} - I_{xz} \dot{r} + qr(I_z - I_y) - I_{xz} pq \\
 M &= I_y \dot{q} + rp(I_x - I_z) + I_{xz}(p^2 - r^2) \\
 N &= -I_{xz} \dot{p} + I_z \dot{r} + pq(I_y - I_x) + I_{xz} qr
 \end{aligned} \tag{38}$$

where

$$\begin{aligned}
 I_x &= \int \int \int (y^2 + z^2) dm \\
 I_y &= \int \int \int (x^2 + z^2) dm \\
 I_z &= \int \int \int (x^2 + y^2) dm \\
 I_{xy} &= \int \int \int xy dm \\
 I_{xz} &= \int \int \int xz dm \\
 I_{yz} &= \int \int \int yz dm
 \end{aligned} \tag{39}$$

where m is the body mass in kg; I_x, I_y, I_z are hexacopter's mass moments of inertia with regard to x, y, and z-axis respectively in kgm^2 ; I_{xz} is the product of inertia. In our simulated plant, the practiced values of the above parameters are as: $m = 3 \text{ kg}$, $I_x = 0.04 \text{ kgm}^2$, $I_y = 0.04 \text{ kgm}^2$, $I_z = 0.06 \text{ kgm}^2$, $I_{xz} = 0 \text{ kgm}^2$.

5.2 Complexities in hexacopter's over-actuated plant dynamics

Unlike the conventional hexacopter plant with 6 degrees of freedom (DOF) rigid body dynamics, 8 DOF over-actuated hexacopter plant with medium fidelity is considered in this work. Two surplus DOF are induced from two moving masses. The masses can slide along their own rail aligned in lengthwise and sideways consecutively. To get a synopsis about the over-actuated simulated Hexacopter plant, its high-level diagram is shown in Fig. 3. The roll and pitch command to the "control mixing" block of Fig. 3 is driven by "attitude controller". In the attitude control mechanism, the inner loop is controlled by a linear PID controller and the outer loop is regulated by PAC. The thrust command of "control mixing" is provided by PAC. Moving of mass to the longitudinal direction shifts the center of gravity (CoG) to X-axis, which is denoted by CG_X in Fig. 3, and CG_Y is expressing the shift of CoG to Y-axis due to the movement of mass to the lateral direction. Both the movements CG_X and CG_Y are controlled by PAC. In control mixing block, a simple linear mixing composition is utilized to convert the roll, pitch, yaw, and thrust commands to the required speed of motors. These signals are used to calculate the required thrust and torque of individual rotor based on the relative airflow faced by each of them and the commanded motor speed. Afterward, the total vertical force and yawing torque of the plant are calculated by summing up the thrust and torque of the individual rotor. The product of thrust to a single rotor and moment arm yields the rolling and pitching moments acting on the hexacopter. Finally, the controlled thrust along with the yawing torque, and rolling and pitching moments are fed to the rigid body dynamics to update the body state accordingly. Hexacopter's detailed rigid body dynamics, nonlinear aerodynamics along with associated complexities are discoursed in the supplementary document.

A user-friendly graphical mask for the rigid body dynamics block allows users to alter the mass, moments of inertia and initial states on demand. During experimentation, errors are obtained by measuring the difference from actual to reference altitude and attitude. These errors, their derivatives, and reference trajectories are intakes for our proposed PAC, which is free from any plant parameters. Therefore, it can operate in a complete model-free manner. Finally, it is important to note that, after manifold simplification as explained in the supplementary document, the employed

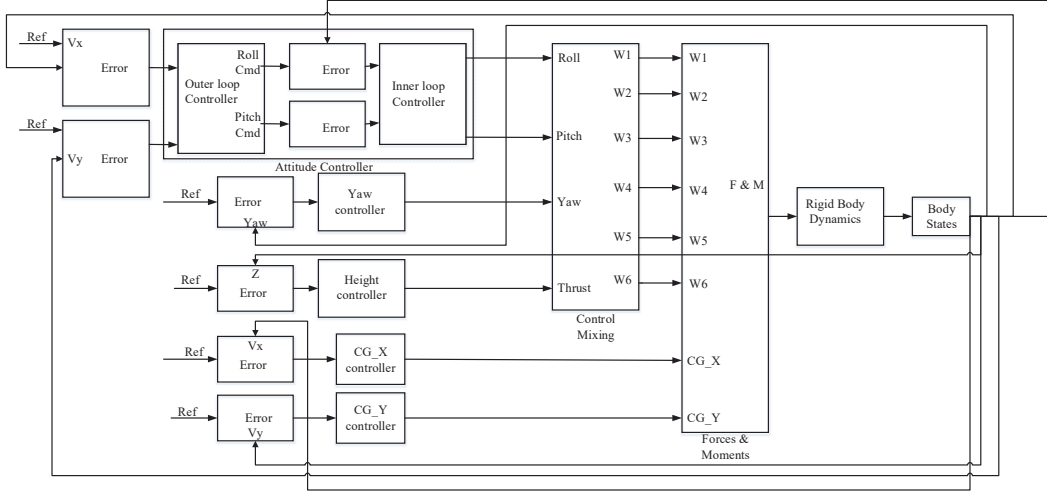


Figure 3: High-level presentation of the over-actuated simulated Hexacopter plant diagram

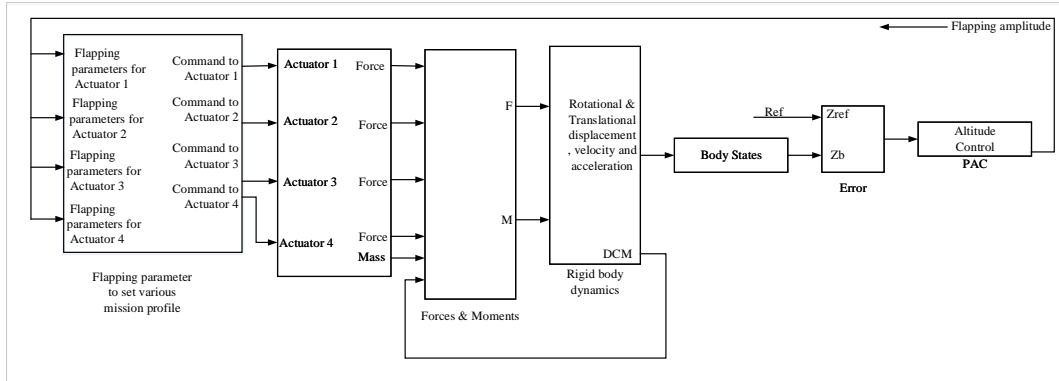


Figure 4: Top level framework of the BI-FWMAV plant

hexacopter dynamics is still highly nonlinear, complex with numerous parameters. Efficient controlling of such plant is difficult for model-based nonlinear controllers or model-free but the parameter-dependent conventional evolving controllers, whereas the premise parameter-free PAC exposes an improved control performance.

5.3 Dynamics of BI-FWMAV plant

Dynamics of the BI-FWMAV plant is highly nonlinear and expresses higher complexity than the hexacopter. It is mainly due to its lightweight and smaller size. The top-level diagram of the simulated BI-FWMAV plant is shown in Fig. 4.

Four wings of the BI-FWMAV is operated by four actuators as exhibited in Fig. 4. From the analysis on dragonfly flight in [49], the influence of seven different flapping parameters on the wings and actuators as well, are considered in developing the BI-FWMAV plant. These parameters are namely stroke plane angle (Fp_{spa})(in rad) , flapping frequency (Fp_{ff}) (in Hz), flapping amplitude (Fp_{fa}) (in rad), mean angle of attack (Fp_{aoa}) (in rad), amplitude of pitching oscillation (Fp_{po}) (in rad), phase difference between the pitching and plunging motion (Fp_{pd}), time step (Fp_{ts}) (in sec). Exploring a variety of combinations of these parameters, the BI-FWMAV can carry out take-off, rolling, pitching, and yawing as explained in [17]. Since our proposed controller is used to regulate the altitude of the BI-FWMAV, it is essential to know the dominant parameter in determining the altitude. After a successful parametric analysis, the flapping amplitude has turned out to be the dominant one in tracking the altitude. Individual forces and moments of actuators are combined to provide the demanded force and moment to the rigid body dynamics based on the relative

airflow acting on each wing and the commanded actuator speed. The combined force utilized in our work can be formulated as follows:

$$F_T = F_{a_1} + F_{a_2} + F_{a_3} + F_{a_4} + (mg \times DCM) \quad (40)$$

where m is the mass, g is the acceleration due to gravity, DCM is the direction cosine matrix, F_{a_i} (where $i = 1, 2, 3, 4$) is the force provided by the individual actuator. Similarly, the total moment necessary for the rigid body can be demonstrated as follows:

$$M_T = M_{a_1} + M_{a_2} + M_{a_3} + M_{a_4} \quad (41)$$

where M_{a_i} (where $i = 1, 2, 3, 4$) is presenting the individual momentum of each wing and can be articulated as

$$M_{a_i} = F_{a_i} \times (CG - CP_i) \quad (42)$$

where $i = 1, 2, 3, 4$; $CG = [0 \ 0 \ 0]$; and $CP_1 = [0.08 \ 0.05 \ 0]$; $CP_2 = [0.08 \ 0.05 \ 0]$; $CP_3 = [0.08 \ -0.05 \ 0]$; $CP_4 = [-0.08 \ -0.05 \ 0]$; and \times is presenting (3×3) cross product. Finally, the accumulated force and moment are transformed into the body coordinate system, and all the required body states like three-dimensional angular displacements (ϕ, θ, ψ) , angular velocities $(\omega_{bx}, \omega_{by}, \omega_{bz})$ and accelerations $(\alpha_{bx} = \frac{d\omega_{bx}}{dt}, \alpha_{by} = \frac{d\omega_{by}}{dt}, \alpha_{bz} = \frac{d\omega_{bz}}{dt})$ and linear displacements (X_b, Y_b, Z_b) , linear velocities (v_{bx}, v_{by}, v_{bz}) and accelerations $(a_{bx} = \frac{dv_{bx}}{dt}, a_{by} = \frac{dv_{by}}{dt}, a_{bz} = \frac{dv_{bz}}{dt})$ are acquired, and the BI-FWMAV states are updated. Complex nonlinear wing dynamics and aerodynamics module of the BI-FWMAV has been clarified in Section 2 of the supplementary document.

From the above discussion, and description of the supplementary document, it is obvious that the BI-FWMAV plant associates profuse parameters with high nonlinearity, though we have omitted some complexity in revealing precise wing kinematics. Deriving a precise mathematical model of such highly nonlinear, complex, and over-actuated plant is exceptionally laborious, where inclusion of uncertainties and uncharted disruption is more complicated or unfeasible in some cases. These perspectives necessitate a controller that performs well with a minimum or no knowledge about the system. Being model-free and self-evolving, our developed PAC is a suitable candidate. More importantly, the impediment of conventional evolving controllers, i.e. involvement of numerous free parameters is resolved here since our controller do not have any premise parameters and only depends upon the consequent parameters namely weights of the network. With such simplistic evolving structure, our proposed controller provides comparable and satisfactory tracking performance.

6 Numerical experiments

In our work, the proposed evolving PAC is used to regulate an over-actuated hexacopter and BI-FWMAV plant, where various altitude and attitude trajectories are tracked for both the MAVs. To be specific, PAC is appraised in tracking altitude of six different trajectories for BI-FWMAV. On the other hand, in hexacopter, the performance of PAC is witnessed both for tracking six different altitudes and sinusoidal attitude, which is detailed in upcoming subsections.

6.1 Experimental results from BI-FWMAV

Our proposed evolving PAC was inspected for numerous tracking signals, and their consequent outcomes were contrasted with a recently developed evolving controller called G-controller [17], a Feed-Forward Neural Network (FFNN) based nonlinear adaptive controller, a Takagi-Sugeno (TS) fuzzy controller, and a PID controller. Our developed PAC's code was written in C programming language and made openly accessible in [21] along with the hexacopter plant to support reproducible research. The performance of all these controllers was observed in BI-FWMAV plant for 100 seconds, where the characteristics of six separate altitude trajectories were as: 1) an unaltered height of 10 meters, can be exposed as $Y_r(t) = 10 \text{ m}$; 2) variable heights with sharp edges, where the heights were altering from 3 m to 6 m after 20 seconds, and then from 6 m to 9 m for another 20 seconds and vice versa, afterward for another 40 seconds. The duration of hovering at a particular height was 20 seconds; 3) variable heights with smooth edges, i.e., the change from one height to another height is not so sharp as the previous trajectory; 4) sum of sines function, which was an amalgamation of a sine wave with a frequency of 0.3 radsec^{-1} , an amplitude of 4 m, and a bias of 6 m, and a cosine wave having a frequency of 0.5 radsec^{-1} , an amplitude of 3 m and a bias of 3 m; 5) a periodic square wave pulse, where the amplitude was varying between 1 m to 11 m, and its frequency is 0.2 radsec^{-1} ; 6) a staircase function, where each step had a duration of 20 seconds. Individual heights of the first three steps are the same as a value of 3 m, which is 2 m in the last step. In these numerical experiments, FFNN based nonlinear adaptive controller operates better than its counterpart PID and TS-fuzzy controllers. Again, both the evolving controllers manifested better tracking

Table 1: Measured features of various controllers in operating the BI-FWMAV (RT: rise time, ST: settling time, CH: constant height, VH: variable height, SS: sum of sine, RMSE: root mean square error, ms: millisecond, m: meter, MA: maximum amplitude, PSW: periodic square wave)

Desired trajectory	Measured features	Control methods				
		PID	FFNN	TS-Fuzzy	G-control	PAC
CH (MA 10 m)	RMSE	0.6460	0.7108	0.6693	0.6631	0.6668
	RT (ms)	50.772	55.828	44.629	41.208	47.207
	ST (ms)	560.98	415.90	222.06	127.15	147.09
	Peak (m)	12.246	11.572	10.451	10.813	10.306
VH with sharp change (MA 9 m)	RMSE	0.3303	0.4078	2.4951	0.3324	0.3561
	RT (ms)	23.931	48.943	43.949	50.892	13.728
	ST (ms)	8176.4	8386.3	8329.4	8133.2	8166.5
	Peak (m)	9.3732	9.6740	9.3010	9.0069	9.2265
VH with smooth change (MA 13 m)	RMSE	0.0895	0.0556	0.0368	0.0228	0.0523
	RT (ms)	8.8573	11.231	1.6537	4.187	0.1314
	ST (ms)	9884.3	9857.7	9871.1	9870.5	9872.1
	Peak (m)	13.006	13.009	13.004	13.019	13.006
SS function (MA 11 m)	RMSE	0.4730	0.5356	0.4631	0.4963	0.5018
	RT (ms)	21.109	31.092	20.616	18.675	19.459
	ST (ms)	9960.1	9960.7	9960.4	9960.1	9960.5
	Peak (m)	11.468	11.502	11.455	11.431	11.462
PSW function (MA 11 m)	RMSE	2.7771	3.3185	499.19	2.5098	2.5115
	RT (ms)	548.93	474.36	2124.3	61.563	59.017
	ST (ms)	9924.1	9911.7	9940.7	9603.2	9634.1
	Peak (m)	12.794	12.573	1030.8	11.007	11.294
Staircase function (MA 12 m)	RMSE	0.3073	0.3791	2.1796	0.2885	0.3072
	RT (ms)	5996.0	4060.7	4015.7	5998.4	6000.3
	ST (ms)	8384.2	8259.1	8094.4	8056.6	8055.1
	Peak (m)	12.453	12.458	12.074	12.007	12.198

performance than the FFNN controller. To acquire a deeper understanding of these manifestations, some of their desired features like root mean squared error (RMSE), rising time (RT) in milliseconds, settling time (ST) in milliseconds, and peak value of the overshoot are captured and tabulated in Table 1. All these anticipations are pictured in Fig. 5 and detailed in the next paragraph.

In Fig. 5 (a), controllers were facilitated to track a 10 m height trajectory, where both from PID and FFNN controller, higher overshoot with peak values more than 12 m were attested. Better performance with peak overshoots of less than 7% of the height was noticed from the TS-fuzzy, and self-adaptive controllers. With regards to peak overshoot, the lowest values were exhibited by evolving controllers in all six different scenarios of Fig. 5, which is evidently signifying the superiority of their evolving structure. Unlike the benchmark evolving G-controller, our proposed one does not consist of any premise parameters. A network with fewer parameters supports PAC to procure prompter settlement, which was witnessed from the lowest settling time of 84.7 seconds in Fig. 5 (a). It was considerably faster than the benchmark evolving G-controller since it demands 127.15 seconds to settle. In most cases of Fig. 5, lowest or very comparative settling time was observed from our proposed controller. The tracking accuracy of the PAC in terms of RMSE and rising time was not always the lowest one. Nonetheless, their achievements were still comparable and sometimes surpassed benchmark controllers.

6.2 Experimental results from hexacopter plant

All the controllers were assessed to track both the altitude and attitude (in terms of rolling and pitching) of the over-actuated hexacopter plant. Six separate trajectories of hexacopter's altitude were as follows: 1) a constant height with a value of 4 m; 2) altering heights with sharp edges, where the peak height was of 9 m; 3) altering heights with smooth edges, where the peak height was of 13 m; 4) a step function, which can be expressed as $3u(t - 3)$, where $u(t)$ is a unit step function; and 5) a staircase function with a peak of 12 m; 6) sum of sines function, which was an amalgamation of a sine wave with a frequency of 0.3 radsec^{-1} , an amplitude of 4 m and a bias of 6 m, and a cosine wave having a frequency of 0.5 radsec^{-1} , an amplitude of 3 m and a bias of 3 m. In all conditions, a higher overshoot was perceived from the PID controller at each sharp changes as depicted in Fig. 6. The peak of this overshoot was lessened while

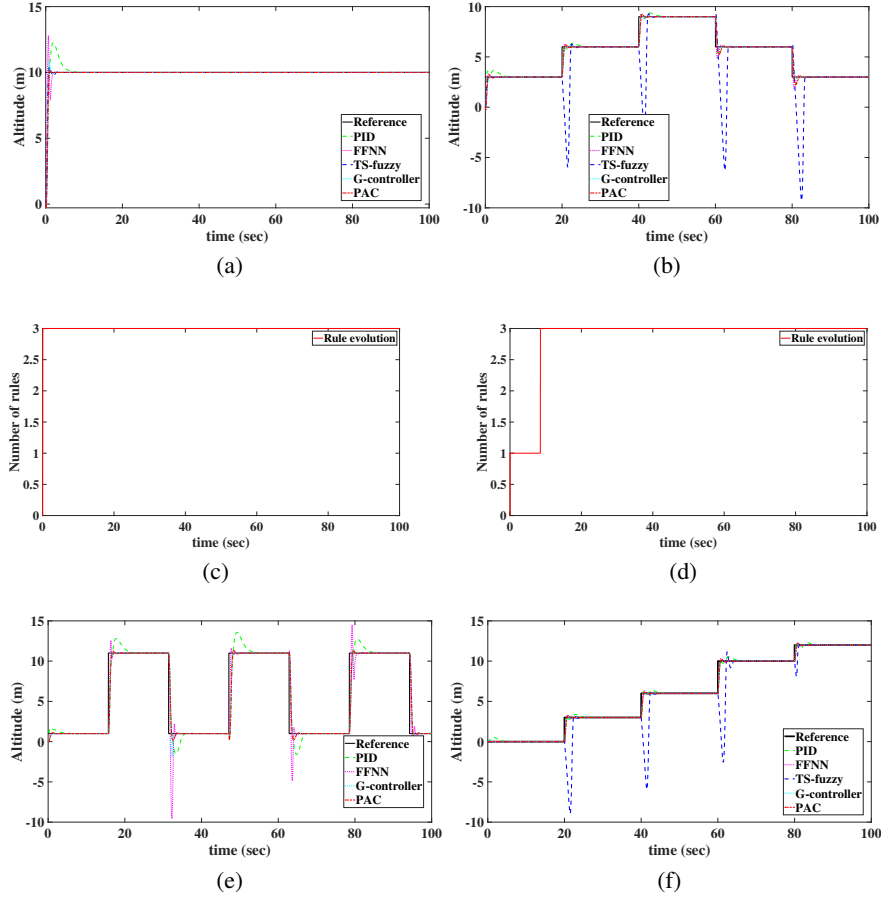


Figure 5: Performance observation of different controllers in tracking altitude of BI-FWMAV, when the trajectories are (a) constant hovering, (b) variable heights with sharp edges, (e) periodic square wave function, (f) staircase function, rule evolution corresponding to (c) constant hovering, (d) variable heights with sharp edges

the PID controller was replaced with the nonlinear adaptive FFNN controller. However, FFNN's performance was not consistent in all cases. Especially in dealing with the square wave trajectory, performance deteriorates significantly as portrayed in Fig.6 (c). This issue was managed by the evolving controllers effectively owing to self-adaptive architecture. Quick settlements were also testified from evolving controllers as recorded in Table 2.

Furthermore, the rolling and pitching position (in rad) was observed with a sum of sine trajectory, which was a fusion of a sine wave with a frequency of 0.3 radsec^{-1} and an amplitude of 0.3 m, and a cosine wave possessing a frequency of 0.5 radsec^{-1} and an amplitude of 0.5 m. The amplitude of the cosine wave was substituted with 0.4 m in tracking the rolling trajectory, where a better tracking was witnessed from the PAC than PID. Interestingly, both the adaptive FFNN controller and TS-fuzzy controller failed to track the rolling trajectory, which is the reason for their absence in Fig. 7 (a). Insertion of PAC yielded better tracking of pitching position, which is obvious from the lowest RMSE of 0.01. The captured RMSE for G-controller was higher, nearly 0.04 as recorded in Table 2.

To sum up, superior or comparative tracking of trajectories were witnessed from our proposed evolving controller. Additionally, faster responses were obtained than the benchmark evolving G-controller, testifying the benefits of having an evolving structure with minimal network parameters.

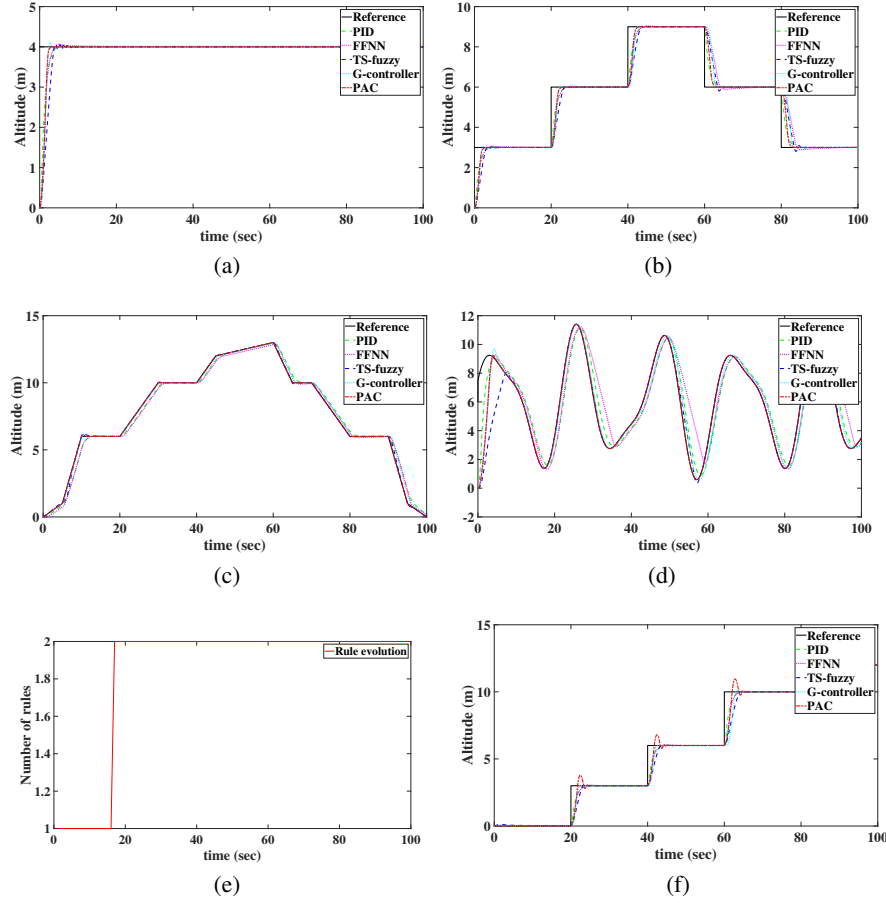


Figure 6: Performance observation of different controllers in tracking altitude of hexacopter, when the trajectories are (a) constant hovering, (b) variable heights with sharp edges, (d) staircase function, (e) variable heights with smooth edges, (f) sum of sines function, and (c) evolution of rules corresponding to constant hovering

6.3 Robustness against uncertainties and noise

In this work, a variety of disturbances were inserted in both BI-FWMAV and hexacopter's plant to verify controllers robustness against those disturbances. For instance, in the plant dynamics of BI-FWMAV, a sudden noise with a peak of 7 m for 0.1 seconds, and the discrete wind gust model Matlab block with a wind velocity 4 m s^{-1} immediately after 2 seconds was embedded in the plant. The mathematical representation of the discrete gust is as follows:

$$V_{wind} = \begin{cases} 0 & x < 0 \\ \frac{V_m}{2} \left(1 - \cos\left(\frac{\pi x}{d_m}\right) \right) & 0 \leq x \leq d_m \\ V_m & x > d_m \end{cases} \quad (43)$$

here V_m is the amplitude of the gust, d_m is denoting the length, x is the traveled-distance, and V_{wind} is the resultant wind velocity in the body axis frame.

Effects of both wind gust and sudden peak noise were observed for all six different altitude trajectories of BI-FWMAV, which are depicted in Fig. 8. From a closer view, obvious performance degradation in dealing with disturbances was witnessed from the non-adaptive PID controller in all cases. In the FFNN controller, due to the adaptation of the network parameters, it performed better than the PID. In some cases, the TS-fuzzy controller performs better than PID. However, its performance was not consistent for all the trajectories. Both FFNN and TS-fuzzy controllers performance deteriorates in tracking trajectories with sharp changes because of the absence of structure adaptation mechanism. On the other hand, sharper settlement and recovery from the adverse effect of gust were sighted from evolving controllers in our experiments. At the same time, in rejecting sudden peak noise, both the PAC and the G-controller dominated

Table 2: Measured features of various controllers in regulating the hexacopter (RT: rise time, ST: settling time, CH: constant height, VH: variable height, ms: millisecond, m: meter, MA: maximum amplitude, PSW: periodic square wave, rad: radian)

Desired trajectory	Measured features	Control method				
		PID	FFNN	TS-fuzzy	G-control	PAC
CH (MA 4 m)	RMSE	0.3551	0.4221	0.4771	0.4239	0.4204
	RT (ms)	208.97	199.15	259.03	141.66	144.63
	ST (ms)	372.82	364.22	368.31	274.51	247.52
	Peak (m)	4.0272	4.0704	4.0714	4.0909	4.0015
VH with sharp change (MA 9 m)	RMSE	0.5574	0.7588	0.7607	0.6491	0.6537
	RT (ms)	205.77	197.21	209.19	122.12	127.84
	ST (ms)	8368.9	8649.9	8412.3	8249.2	8279.0
	Peak (m)	9.0281	9.0406	9.0216	9.0022	9.0010
VH with smooth change (MA 13 m)	RMSE	0.3642	0.3651	0.1013	0.0273	0.0268
	RT (ms)	122.21	144.33	6.7804	5.2776	2.4948
	ST (ms)	9932.5	9938.4	9869.4	9929.0	9927.0
	Peak (m)	12.987	12.868	13.007	12.999	13.002
Step function (MA 3 m)	RMSE	0.2420	0.2795	0.3078	0.2842	0.2834
	RT (ms)	203.94	197.22	215.14	121.83	112.14
	ST (ms)	445.12	432.87	396.36	300.50	451.29
	Peak (m)	3.0289	3.0676	3.0394	3.0040	3.6242
Staircase function (MA 12 m)	RMSE	0.5221	0.6151	0.6959	0.5999	0.6237
	RT (ms)	6019.9	6030.9	5970.0	6004.2	4227.9
	ST (ms)	8245.3	8285.4	8212.7	8179.5	8391.5
	Peak (m)	12.026	12.039	12.017	11.998	12.587
Sum of sine function (MA 11 m)	RMSE	1.2270	1.7091	1.2636	1.0956	1.0856
	RT (ms)	59.638	114.04	165.62	125.94	122.53
	ST (ms)	10050	10009	9955.6	10004	10210
	Peak (m)	11.129	11.235	11.426	11.413	11.409
Pitching	RMSE	0.3513	0.0451	N/A	0.0466	0.0109
	RT (ms)	14.907	14.686	N/A	65.469	10.135
	ST (ms)	10057	10057	N/A	9982.9	10053
	Peak (rad)	0.5615	0.5758	N/A	0.5398	0.5469
Rolling	RMSE	0.1673	N/A	N/A	0.0290	0.0259
	RT (ms)	166.116	N/A	N/A	118.75	91.596
	ST (ms)	10037	N/A	N/A	9978.9	9979.9
	Peak (rad)	0.3907	N/A	N/A	0.3513	0.4852

other benchmark controllers, where the lowest peaks were witnessed from them. Such accomplishments were possible due to their evolving structure with an adaptation of fewer parameters than the benchmark controllers.

In the hexacopter dynamics, a sharp peak noise with an amplitude of 2 m for 0.1 seconds was implanted to observer robustness of the controllers. Effects of disturbance were witnessed for four different altitude trajectories of hexacopter. RMSE, settling time, rise time and peak overshoot values for all those trajectories were tabulated for all benchmark and proposed controller in Table 4. Such perturbation was handled effectively by evolving controllers than their static counterparts as attested in Fig. 9. A high peak and slow settlement were detected in PID, TS-fuzzy and FFNN controllers. On the contrary, a negligible overshoot with a rapid settlement was inspected from the evolving controllers. For example, after closely observing the constant altitude trajectory in Fig. 9 (c), recorded values of rising time were less than 6 ms from the evolving controllers, which was more than 100 ms in FFNN and PID controllers. A similar phenomenon was observed in remaining trajectories, which is evidently declaring the improved robustness against uncertainties of the PAC in contrast with the benchmark static controller.

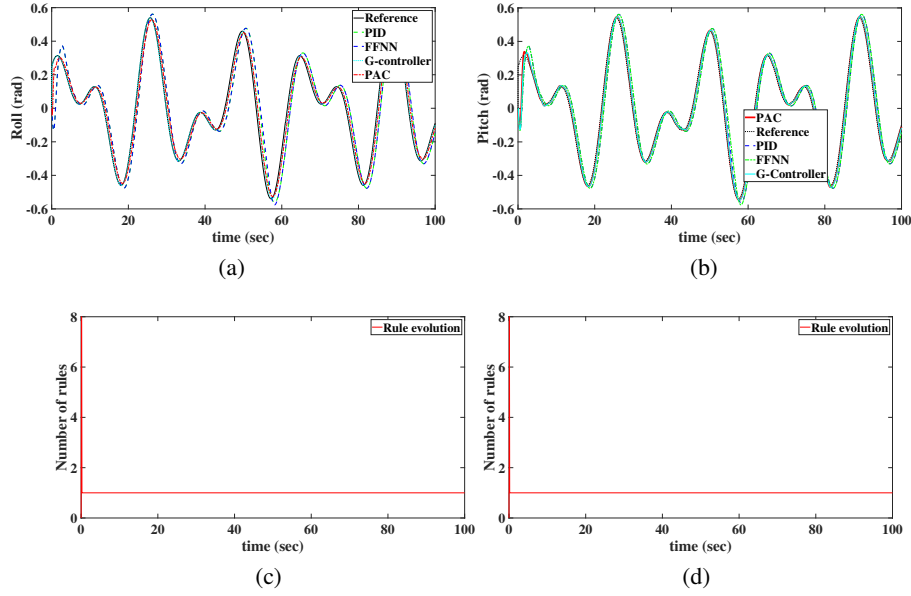


Figure 7: Performance observation of different controllers in tracking desired (a) rolling, (b) pitching of the hexacopter MAV, (c) evolution of rules in tracking rolling, and (d) pitching in hexacopter

Table 3: Measured features of various controllers in operating the BI-FWMAV by considering a noise of sudden peak amplitude, and wind gust disturbance (RT: rise time, ST: settling time, CH: constant height, VH: variable height, SS: sum of sine, ms: millisecond, m: meter, MA: maximum amplitude, PSW: periodic square wave)

Desired trajectory	Measured features	Control method				
		PID	FFNN	TS-fuzzy	G-control	PAC
CH (MA 10 m)	RMSE	0.6536	0.7268	0.5746	0.6657	0.6712
	RT (ms)	50.772	55.828	44.629	41.208	47.207
	ST (ms)	1025.9	2707.2	743.39	635.53	747.43
	Peak (m)	12.247	11.573	11.035	11.022	11.035
VH with sharp change (MA 9 m)	RMSE	0.3430	0.4237	2.4603	0.3351	0.3611
	RT (ms)	23.931	48.943	43.949	50.892	13.728
	ST (ms)	8176.2	8386.3	8329.4	8133.2	8166.5
	Peak (m)	9.3731	9.6742	9.3010	9.0073	9.2270
VH with smooth change (MA 13 m)	RMSE	0.1258	0.1541	0.0823	0.0613	0.0899
	RT (ms)	8.8573	11.231	1.6537	4.1881	0.1314
	ST (ms)	9884.3	9857.5	9871.1	9870.5	9872.1
	Peak (m)	13.007	13.009	13.004	13.019	13.006
SS function (MA 11 m)	RMSE	0.4832	0.5565	0.4685	0.4998	0.5075
	RT (ms)	21.109	31.092	20.616	18.675	19.459
	ST (ms)	9960.1	9959.7	9960.1	9959.8	9960.1
	Peak (m)	11.468	11.712	11.518	11.489	11.534
PSW function (MA 11 m)	RMSE	2.7739	3.2660	421.39	2.5112	2.5122
	RT (ms)	546.47	472.35	1040.5	57.067	59.508
	ST (ms)	9923.9	9911.7	9972.2	9603.2	9634.1
	Peak (m)	12.794	12.667	736.93	12.067	12.073
Staircase function (MA 12 m)	RMSE	0.3205	0.3960	2.1397	0.2916	0.3131
	RT (ms)	5996.0	4067.3	4024.4	5999.4	6002.2
	ST (ms)	8370.8	8156.2	8094.8	8056.5	8055.1
	Peak (m)	12.453	12.458	12.072	12.007	12.198

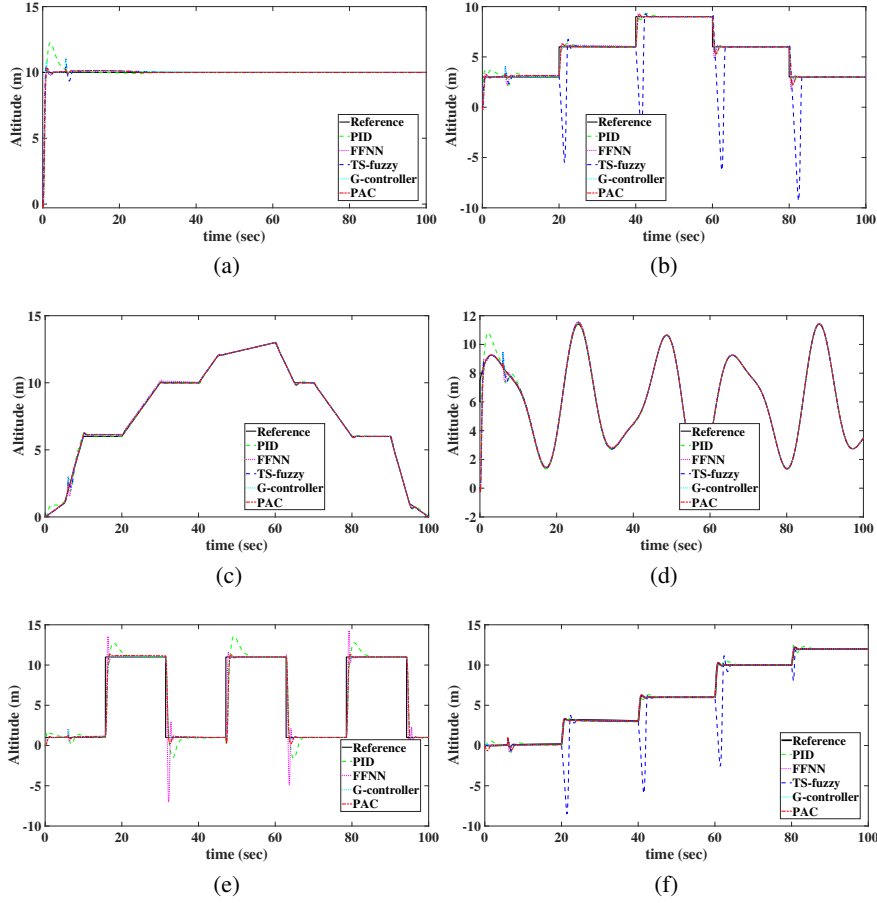


Figure 8: Performance observation of different controllers in tracking altitude of BI-FWMAV by considering a sudden noise, and wind gust uncertainty, when the trajectories are (a) constant hovering, (b) variable heights with sharp edges, (c) variables height with smooth edges, (d) sum of sine function, (e) periodic square wave function, and (f) staircase function

6.4 Self-adaptive mechanism of PAC

Based on the bias-variance concept explained in section 4, rules of the PAC have been evolved dynamically in different experiments. Before analyzing the evolution of the structure of our proposed controller, we have tried to summarize shortfalls of the benchmark controllers used in this work. The linear PID controller’s realization is based upon three gain parameters, namely proportional, integral, and differential gain. They are typically denoted as K_p , K_i , and K_D . It requires to set values for those parameters in offline before utilizing in control operation, which may oblige repetitious efforts. Besides, those parameters can not be tuned online. Before performing the control operation, both the adaptive FFNN and TS-fuzzy controllers require offline training encouraged by the PID controller’s input-output datasets. Though they adapt their network parameters during operation, they have a fixed structure with a hidden layer consists of ten fixed nodes and five rules. To attain more robustness against disturbances, the benchmark G-controller can adapt both the network and parameters. Nonetheless, it needs to deal with lots of free parameters in both antecedent and consequent parts. Besides, the evolution of G-controller is regulated by some user-defined thresholds. Sometimes, it is causing a large settling time. On the contrary, our proposed evolving controller has no premise parameters. The only parameter that needs to be adapted is weight, which is adapted here using SMC theory. Unlike the benchmark evolving controllers, PAC is free from predefined problem-dependent parameter for regulating its structure.

The structure evolution in terms of added or pruned rules for some trajectories of BI-FWMAV and hexacopter was disclosed graphically in Fig. 5 (c) and (d), Fig. 6 (c), and in Fig. 7 to get a vivid insight into the evolution of rules in

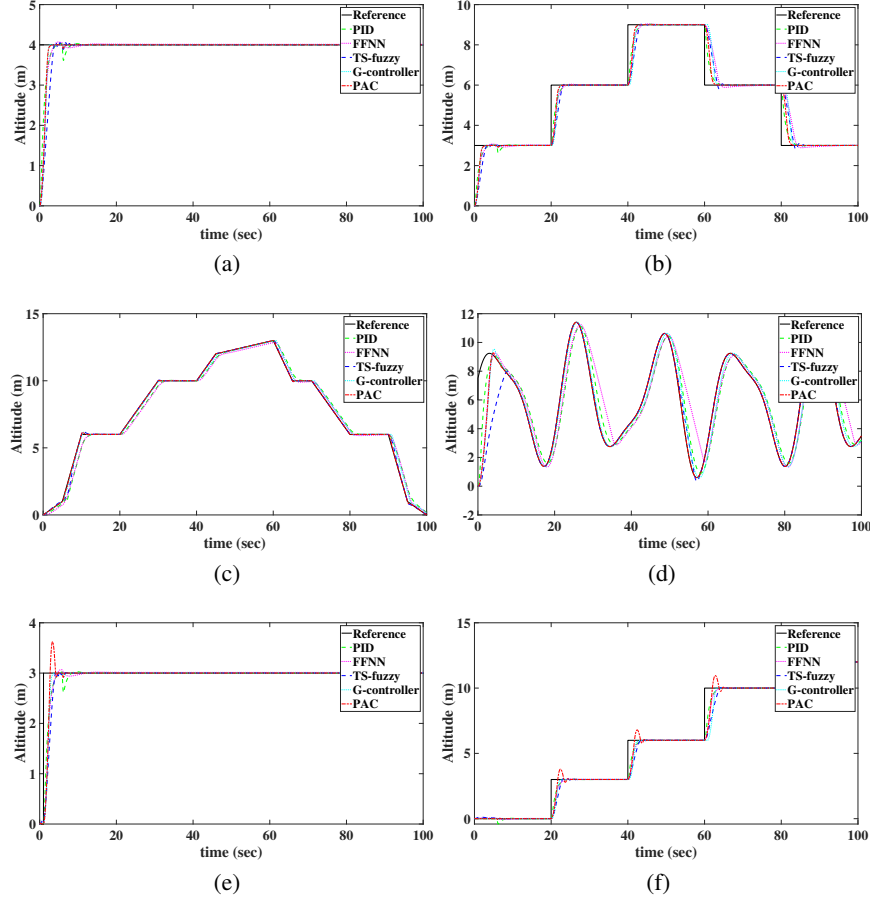


Figure 9: Performance observation of different controllers in tracking altitude of hexacopter considering sudden noise, when the trajectories are (a) constant hovering, (b) variable heights with sharp edges, (c) variable heights with smooth edges, (d) sum of sines function, (e) step function, and (f) staircase function

PAC. For further clarification, the fuzzy rule extracted by PAC in controlling the BI-FWMAV can be uttered as follows:

$$R^1 : \text{IF } X_n \text{ is close to } \left([1, e, \dot{e}, y_r] \times [0.0121, 0.0909, 0.4291, 0.6632]^T \right), \quad (44)$$

$$\text{THEN } y = 0.0121 + 0.0909e + 0.4291\dot{e} + 0.6632y_r$$

where e is the error, i.e., the difference between the reference and actual output of the plant, \dot{e} is the error derivative, i.e., the difference between the present and previous state error value, y_r is the reference for the plant to be controlled. Since PAC is targeted to minimize the tracking error to zero or very close to zero, it needs information about the error as an input to the closed-loop system. It is also witnessed in PAC's rule as exposed in (44). When PAC was controlling the BI-FWMAV in tracking a constant altitude of 10 m, it generated 3 rules within 1 second at the beginning of control operation. Since the reference was unaltered and stability of the plant was achieved, PAC did not add or prune any extra rule later on as witnessed from the Fig. 5 (c). While BI-FWMAV was following a variable height trajectory with sharp changes at edges, the PAC started operating by producing only one rule. After 8 seconds it added two more rules and achieved system stability. After that, the changes in trajectories were handled by PAC through the tuning of weights only. It does not need any further structure evolution as observed in Fig. 5 (d). The successful evolution of rules by confirming system stability was also achieved by PAC in controlling the hexacopter plant. For instance, PAC supported hexacopter to track a constant altitude of 4 m with two rules as displayed in Fig. 6 (c). While PAC was regulating the rolling of hexacopter for a sum of sine trajectory, it started operating with only one rule. Immediately after 17 seconds, it added another two rules, however, one of them was pruned at 19 seconds to minimize the overfitting phenomenon, while maintained system stability with two rules only. With these two rules, it tracked the trajectory efficiently through the SMC based weight adaptation. A similar scenario was witnessed in controlling the pitching position of the hexacopter since the same trajectory was employed. In sum up, by adapting both the structure and

Table 4: Measured features of various controllers in regulating the hexacopter by considering noise of sudden peak amplitude (RT: rise time, ST: settling time, CH: constant height, VH: variable height, ms: millisecond, m: meter, MA: maximum amplitude)

Desired trajectory	Measured features	Control method				
		PID	FFNN	TS-fuzzy	G-control	PAC
CH (MA 4 m)	RMSE	0.3383	0.4067	0.4772	0.4237	0.4048
	RT (ms)	208.28	197.14	259.03	141.66	144.67
	ST (ms)	746.30	831.62	634.67	274.51	623.97
	Peak (m)	4.0293	4.0704	4.0714	4.0909	4.0015
VH with sharp change (MA 9 m)	RMSE	0.5367	0.7586	0.7479	0.6509	0.6391
	RT (ms)	203.76	195.22	209.19	122.12	125.84
	ST (ms)	8315.9	8583.9	8411.8	8257.2	8232.0
	Peak (m)	9.0281	9.0406	9.0258	9.0022	9.0010
VH with smooth change (MA 13 m)	RMSE	0.3788	0.3666	0.1189	0.0322	0.0281
	RT (ms)	110.21	142.33	6.7867	5.2776	2.4948
	ST (ms)	9879.5	9877.4	9869.2	9940.0	9871.0
	Peak (m)	12.987	12.868	13.005	13.008	13.002
Step function (MA 3 m)	RMSE	0.2439	0.2795	0.3078	0.2841	0.2834
	RT (ms)	203.94	197.23	215.13	121.83	112.14
	ST (ms)	763.38	912.24	396.34	300.48	631.1784
	Peak (m)	3.0285	3.0676	3.0394	3.0042	3.6242
Staircase function (MA 12 m)	RMSE	0.5074	0.6000	0.6961	0.5998	0.6078
	RT (ms)	5993.9	5980.9	5973.7	6004.0	4144.9
	ST (ms)	8204.3	8222.4	8212.7	8183.5	8254.5
	Peak (m)	12.028	12.039	12.021	11.998	12.587
Sum of sine function (MA 11 m)	RMSE	1.2123	1.7003	1.4325	1.0954	1.0787
	RT (ms)	59.638	114.03	181.41	125.94	122.53
	ST (ms)	9945.9	9944.2	9959.2	10004	9959.7
	Peak (m)	11.130	11.235	11.400	11.413	11.409
Pitching	RMSE	0.3513	0.0451	N/A	0.0466	0.0109
	RT (ms)	14.907	14.686	N/A	65.469	10.135
	ST (ms)	10057	10057	N/A	9982.9	10053
	Peak (rad)	0.5615	0.5758	N/A	0.5398	0.5469
Rolling	RMSE	0.1673	N/A	N/A	0.0290	0.0259
	RT (ms)	166.116	N/A	N/A	118.75	91.596
	ST (ms)	10037	N/A	N/A	9978.9	9979.9
	Peak (rad)	0.3907	N/A	N/A	0.3513	0.4852

weights, the PAC was controlling the MAVs effectively to follow the desired trajectories very closely and by preserving the stability of the closed-loop system.

6.5 PAC's performance analysis using the Wilcoxon signed-rank test

As a simple statistical test, Wilcoxon signed-rank tests had been performed among various controllers. In these tests, the residual error among the reference trajectories and plant's actual trajectories are calculated for all the utilized controllers. To do the Wilcoxon signed-rank test, the Matlab function, namely *signrank* has been utilized as follows:

$$[p, h] = \text{signrank}(A, B) \quad (45)$$

where A is indicating the dataset of residual error from our proposed PAC, and B is denoting the dataset of residual error from the benchmark controllers. The test expressed in Eq. (45) is returning a logical value that indicates the test decision. Theoretically, $h = 1$ is expressing a rejection of the null hypothesis, whereas $h = 0$ is pointing the opposite at the 5% significance level. In other words, when A differs statistically from B , then $h = 1$. When $h = 0$, A and B are statistically similar to each other.

In this work, from the Wilcoxon signed-rank test between the PAC (considered as A) and a benchmark controller (considered as B), we have observed the value of h . It gives us better insight regarding our proposed controller's

Table 5: Wilcoxon signed rank test between controllers in regulating the altitude of MAVs

Plant	Desired trajectory	Controllers	RMSE	h
BI-FWMAV	CH (MA 10 m)	PID	0.6460	0
		PAC	0.6668	
		TS-Fuzzy	0.6693	1
		PAC	0.6668	
		FFNN	0.7108	1
		PAC	0.6668	
		G-controller	0.6631	0
		PAC	0.6668	
Hexacopter	CH (MA 4 m)	PID	0.3551	0
		PAC	0.4204	
		TS-Fuzzy	0.4771	1
		PAC	0.4204	
		FFNN	0.4221	0
		PAC	0.4204	
		G-controller	0.4239	0
		PAC	0.4204	

performance, which is explained in this paragraph. We already have recorded the RMSE of all the controllers for various trajectory tracking performance. When the RMSE of the PAC is lower than the benchmark one, it is indicating the superiority of PAC over benchmark controllers. It is supported by the logical value of $h = 1$ since the residual error dataset of PAC is statistically different and lower than the benchmark controllers. On the other hand, when the RMSE is lower in a benchmark controller than the PAC, the logical value of h is 0. It is indicating a comparable performance of the PAC with regards to the benchmark ones since both of their residual error datasets are very similar. To get a clearer view, the constant height trajectory tracking performance with the Wilcoxon signed-rank test for both the plants are tabulated in Table 5.

The observation from Table 5 can be summarized in three different cases as follows: 1) In case of superior performance from the PAC, i.e., when the RMSE is lower in PAC than the benchmark one, the logical value of h is 1. It indicates that the residual error set of PAC is different from the benchmark controller. Therefore, different residual error sets with lower RMSE is clearly indicating the improved performance of the PAC; 2) When the performance of the benchmark controllers are better than the PAC by having a slightly lower RMSE, the value of h is 0. It is indicating similar residual error sets from both the benchmark controller and PAC. Thus, the performance of PAC is comparable with the benchmark one; 3) In case, the performance of PAC is slightly better than the benchmark controllers. However, the value of h is 0, which is stating a comparable performance from the benchmark controllers. The Wilcoxon signed-rank test results for all other trajectories are attached in the supplementary document.

6.6 Comparison against closely related work

To revile the strength of the proposed controller, namely PAC against its closely related recent variants, a comparison among them is addressed in this subsection. The mechanism of growing and pruning rules and control laws of these controllers are compared here. To get a clearer overview, they are tabulated in Table 6.

In closely-related evolving controllers, mostly univariate or multivariate Gaussian membership functions are employed in the antecedent part, where they need to tune the antecedent parameters like centers and widths. Unlike them, hyperplane-based clustering technique is used in PAC, where it does not have any antecedent parameters. Therefore, PAC is free from the computation of tuning of such parameters. Besides, all the above-mentioned controllers have a dependency on predefined thresholds to grow or prune rules. To get rid of such dependence on predefined values, in our PAC, the concept of bias and variance has been incorporated.

7 Conclusion

Based on the research gap in controlling MAVs in cluttered environments, a completely model-free evolving controller, namely PAC is proposed in this work. A bottleneck of the existing evolving controllers is the utilization of numerous free parameters and their online adaptation. Such inadequacy has been mitigated in our PAC since it has no premise

Table 6: Comparison against closely related work

Algorithm	Rule-growing method	Rule-pruning method	Clustering technique and control laws
G-controller [17]	The datum significance method	The extended rule significance method	Multivariate Gaussian membership function is utilized in the antecedent part, which creates hyper-ellipsoidal clusters. SMC-based adaptation laws are used.
eTS controller [12]	Spatial proximity between a particular data point and all other points, namely potential is used to add rules.	No rule pruning mechanism.	The Gaussian membership function is used in the antecedent part, which creates hyper-spherical clusters. Recursive least-square-based adaptation laws are used.
Adaptive fuzzy neural controller [13]	ϵ -completeness and system error are measured to add rules.	Error reduction ratio (ERR) is utilized to prune a rule.	The Gaussian membership function is used in the antecedent part, which creates hyper-spherical clusters. Tracking error-based parameter adaptation laws are employed.
Interval type-2 fuzzy brain emotional learning control (T2FBELC) [50]	Maximum membership grade of input is measured to add rules	Minimum membership grade is calculated to delete rules.	The Gaussian membership function is used in the antecedent part, which creates hyper-spherical clusters. The steepest descent gradient approach is used to derive adaptation laws.

parameters. The only parameter used in our evolving controller to acquire the desired tracking is the weight. For instance, in our experiment, the benchmark evolving G-controller with three rules requires 48 network parameters, whereas PAC needs only 12 parameters with three rules. Apart from that, conventional evolving controllers adhere to user-defined problem-based thresholds to shape their structure. In PAC, rather than predefined parameters, the bias-variance concept based network significance method is utilized to determine its structure. The PAC has been verified by implementing them in various MAV plants namely BI-FWMAV and hexacopter to track diverse trajectories. All the achievements are contrasted with a commonly utilized PID controller, an adaptive nonlinear FFNN controller, a TS-fuzzy controller, an evolving controller namely G-controller. Furthermore, the controller's robustness against uncertainties and disruptions is ascertained by injecting a wind gust and sudden peak to the MAVs dynamics. In controlling both plants with uncertainties, lower or comparable overshoot and settling time were observed from PAC with a simplified evolving structure, which is testifying its robustness against uncertainties and compatibility in regulating MAVs. Inspired by PAC's efficient performance in controlling the simulated BI-FWMAV and hexacopter plant, it will be employed in MAVs hardware in the future. Besides, we will be continuing to develop evolving fuzzy controllers with fewer network parameters by maintaining satisfactory performance.

Acknowledgment

The authors would like to thank the unmanned aerial vehicle laboratory of the UNSW Canberra for supporting with the BI-FWMAV and hexacopter plants, and the computational support from the Computational Intelligence Laboratory of Nanyang Technological University (NTU) Singapore. The 5th author acknowledges the support by the COMET-K2 Center of the Linz Center of Mechatronics (LCM) funded by the Austrian federal government and the federal state of Upper Austria. This work was financially supported by the NTU start-up grant and MOE Tier-1 grant.

References

- [1] Md Meftahul Ferdous, Sreenatha G Anavatti, Mahardhika Pratama, and Matthew A Garratt. Towards the use of fuzzy logic systems in rotary wing unmanned aerial vehicle: a review. *Artificial Intelligence Review*, pages 1–34, 2018.
- [2] Patricia Melin, Alejandra Mancilla, Miguel Lopez, and Olivia Mendoza. A hybrid modular neural network architecture with fuzzy sugeno integration for time series forecasting. *Applied Soft Computing*, 7(4):1217–1226, 2007.
- [3] Patricia Melin and Oscar Castillo. Adaptive intelligent control of aircraft systems with a hybrid approach combining neural networks, fuzzy logic and fractal theory. *Applied Soft Computing*, 3(4):353–362, 2003.
- [4] Patricia Melin and Oscar Castillo. An intelligent hybrid approach for industrial quality control combining neural networks, fuzzy logic and fractal theory. *Information Sciences*, 177(7):1543–1557, 2007.
- [5] Patricia Melin and Oscar Castillo. A new method for adaptive control of non-linear plants using type-2 fuzzy logic and neural networks. *International Journal of General Systems*, 33(2-3):289–304, 2004.
- [6] Emanuel Ontiveros-Robles, Patricia Melin, and Oscar Castillo. Comparative analysis of noise robustness of type 2 fuzzy logic controllers. *Kybernetika*, 54(1):175–201, 2018.
- [7] Oscar Castillo, Leticia Cervantes, Jose Soria, Mauricio Sanchez, and Juan R Castro. A generalized type-2 fuzzy granular approach with applications to aerospace. *Information Sciences*, 354:165–177, 2016.
- [8] Oscar Castillo, Leticia Amador-Angulo, Juan R Castro, and Mario Garcia-Valdez. A comparative study of type-1 fuzzy logic systems, interval type-2 fuzzy logic systems and generalized type-2 fuzzy logic systems in control problems. *Information Sciences*, 354:257–274, 2016.
- [9] Leticia Cervantes and Oscar Castillo. Type-2 fuzzy logic aggregation of multiple fuzzy controllers for airplane flight control. *Information Sciences*, 324:247–256, 2015.
- [10] Mauricio A Sanchez, Oscar Castillo, and Juan R Castro. Generalized type-2 fuzzy systems for controlling a mobile robot and a performance comparison with interval type-2 and type-1 fuzzy systems. *Expert Systems with Applications*, 42(14):5904–5914, 2015.
- [11] Wen-Jer Chang, Hong-Yu Qiao, and Cheung-Chieh Ku. Sliding mode fuzzy control for nonlinear stochastic systems subject to pole assignment and variance constraint. *Information Sciences*, 432:133–145, 2018.
- [12] Plamen Angelov. A fuzzy controller with evolving structure. *Information Sciences*, 161(1-2):21–35, 2004.
- [13] Yang Gao and Meng Joo Er. Online adaptive fuzzy neural identification and control of a class of MIMO nonlinear systems. *IEEE Transactions on Fuzzy Systems*, 11(4):462–477, 2003.

- [14] Plamen P Angelov and Dimitar P Filev. An approach to online identification of Takagi-Sugeno fuzzy models. *IEEE Transactions on Systems, Man, and Cybernetics, Part B (Cybernetics)*, 34(1):484–498, 2004.
- [15] Jean-Camille de Barros and Arthur L Dexter. Evolving fuzzy model-based adaptive control. In *IEEE International Fuzzy Systems Conference, 2007. FUZZ-IEEE 2007*, pages 1–5. IEEE, 2007.
- [16] Hong-Gui Han, Xiao-Long Wu, and Jun-Fei Qiao. Real-time model predictive control using a self-organizing neural network. *IEEE Transactions on Neural Networks and Learning Systems*, 24(9):1425–1436, 2013.
- [17] Md Meftahul Ferdous, Mahardhika Pratama, Sreenatha Anavatti, Matthew A Garratt, and Yongping Pan. Generic evolving self-organizing neuro-fuzzy control of bio-inspired unmanned aerial vehicles. *IEEE Transactions on Fuzzy Systems*, 2019.
- [18] Igor Škrjanc, Sašo Blazic, and Plamen Angelov. Robust evolving cloud-based pid control adjusted by gradient learning method. In *2014 IEEE Conference on Evolving and Adaptive Intelligent Systems (EAIS)*, pages 1–8, 2014.
- [19] Md Meftahul Ferdous, Mahardhika Pratama, Sreenatha Anavatti, and Matthew A Garratt. PALM: An Incremental Construction of Hyperplanes for Data Stream Regression. *IEEE Transactions on Fuzzy Systems*, 2019.
- [20] Mahardhika Pratama, Choiru Za'in, Andri Ashfahani, Yew Soon Ong, and Weiping Ding. Automatic construction of multi-layer perceptron network from streaming examples. In *The 28th ACM International Conference on Information and Knowledge Management*. ACM, 2019.
- [21] Md Meftahul Ferdous and Mahardhika Pratama. Evolving controller PAC, 2018.
- [22] Samir Bouabdallah, Andre Noth, and Roland Siegwart. PID vs LQ control techniques applied to an indoor micro quadrotor. In *Proc. of The IEEE International Conference on Intelligent Robots and Systems (IROS)*, pages 2451–2456. IEEE, 2004.
- [23] Satcha Busarakum and Varawan Srichatrapimuk. The design of sliding mode control of a hexarotor. In *2014 IEEE Conference on Systems, Process and Control (ICSPC)*, pages 47–52. IEEE, 2014.
- [24] Jan Bacik, Daniela Perdukova, and Pavol Fedor. Design of fuzzy controller for hexacopter position control. In *Artificial Intelligence Perspectives and Applications*, pages 193–202. Springer, 2015.
- [25] Byoung S Kim and Anthony J Calise. Nonlinear flight control using neural networks. *Journal of Guidance, Control, and Dynamics*, 20(1):26–33, 1997.
- [26] Sefer Kurnaz, Omer Cetin, and Okyay Kaynak. Adaptive neuro-fuzzy inference system based autonomous flight control of unmanned air vehicles. *Expert Systems with Applications*, 37(2):1229–1234, 2010.
- [27] Xiangjian Chen, Di Li, Zhijun Xu, and Yue Bai. Robust control of quadrotor MAV using self-organizing interval type-II fuzzy neural networks (SOIT-IIFNNs) controller. *International Journal of Intelligent Computing and Cybernetics*, 4(3):397–412, 2011.
- [28] Cheng Dong, Ning Wang, and Meng Joo Er. Self-organizing adaptive robust fuzzy neural attitude tracking control of a quadrotor. In *2016 35th Chinese Control Conference (CCC)*, pages 10724–10729. IEEE, 2016.
- [29] I Škrjanc, J Iglesias, A Sanchis, D Leite, E. D Lughofer, and F Gomide. Evolving fuzzy and neuro-fuzzy approaches in clustering, regression, identification, and classification: A survey. *Information Sciences*, 490:344–368, 2019.
- [30] Chih-Min Lin and Te-Yu Chen. Self-organizing CMAC control for a class of MIMO uncertain nonlinear systems. *IEEE Transactions on Neural Networks*, 20(9):1377–1384, 2009.
- [31] Andon V Topalov, Kwang-Choon Kim, Jong-Hwan Kim, and Bong-Kuk Lee. Fast genetic on-line learning algorithm for neural network and its application to temperature control. In *Evolutionary Computation, 1996., Proceedings of IEEE International Conference on*, pages 649–654. IEEE, 1996.
- [32] Chia-Feng Juang and Chin-Teng Lin. An online self-constructing neural fuzzy inference network and its applications. *IEEE Transactions on Fuzzy Systems*, 6(1):12–32, 1998.
- [33] Mahardhika Pratama, Sreenatha G Anavatti, Plamen P Angelov, and Edwin Lughofer. PANFIS: A novel incremental learning machine. *IEEE Transactions on Neural Networks and Learning Systems*, 25(1):55–68, 2014.
- [34] Richard J Hathaway and James C Bezdek. Switching regression models and fuzzy clustering. *IEEE Transactions on Fuzzy Systems*, 1(3):195–204, 1993.
- [35] Euntai Kim, Minkee Park, Seunghwan Ji, and Mignon Park. A new approach to fuzzy modeling. *IEEE Transactions on Fuzzy Systems*, 5(3):328–337, 1997.
- [36] Wen Zou, Chaoshun Li, and Nan Zhang. A T-S Fuzzy Model Identification Approach based on a Modified Inter Type-2 FRCM Algorithm. *IEEE Transactions on Fuzzy Systems*, 2017.

- [37] wolfram. Point-plane distance, 2018.
- [38] Andri Ashfahani, Mahardhika Pratama, Edwin Lughofer, and Yew Soon Ong. Devdan: Deep evolving denoising autoencoder. *to appear in Neurocomputing*, 2019.
- [39] João Gama, Ricardo Fernandes, and Ricardo Rocha. Decision trees for mining data streams. *Intelligent Data Analysis*, 10(1):23–45, 2006.
- [40] João Gama, Indrè Žliobaitė, Albert Bifet, Mykola Pechenizkiy, and Abdelhamid Bouchachia. A survey on concept drift adaptation. *ACM Computing Surveys (CSUR)*, 46(4):44, 2014.
- [41] Erdal Kayacan, Ozkan Cigdem, and Okyay Kaynak. Sliding mode control approach for online learning as applied to type-2 fuzzy neural networks and its experimental evaluation. *IEEE Transactions on Industrial Electronics*, 59(9):3510–3520, 2012.
- [42] Vadim I Utkin. *Sliding modes in control and optimization*. Springer Science & Business Media, 2013.
- [43] Erdal Kayacan and Reinaldo Maslim. Type-2 Fuzzy Logic Trajectory Tracking Control of Quadrotor VTOL Aircraft With Elliptic Membership Functions. *IEEE/ASME Transactions on Mechatronics*, 22(1):339–348, 2017.
- [44] L-X Wang. Stable adaptive fuzzy control of nonlinear systems. *IEEE Transactions on Fuzzy Systems*, 1(2):146–155, 1993.
- [45] Rolf Rysdyk and Anthony Calise. Fault tolerant flight control via adaptive neural network augmentation. In *Guidance, Navigation, and Control Conference and Exhibit*, page 4483, 1998.
- [46] JM Kok and JS Chahl. A low-cost simulation platform for flapping wing MAVs. In *SPIE Smart Structures and Materials+ Nondestructive Evaluation and Health Monitoring*, pages 94290L–94290L. International Society for Optics and Photonics, 2015.
- [47] Z Jane Wang and David Russell. Effect of forewing and hindwing interactions on aerodynamic forces and power in hovering dragonfly flight. *Physical Review Letters*, 99(14):148101, 2007.
- [48] Robert C Nelson. *Flight stability and automatic control*, volume 2. WCB/McGraw Hill New York, 1998.
- [49] JM Kok and JS Chahl. Systems-level analysis of resonant mechanisms for flapping-wing flyers. *Journal of Aircraft*, 51(6):1833–1841, 2014.
- [50] Tien-Loc Le, Chih-Min Lin, and Tuan-Tu Huynh. Self-evolving type-2 fuzzy brain emotional learning control design for chaotic systems using PSO. *Applied Soft Computing*, 73:418–433, 2018.